SQANTI-reads: a tool for the quality assessment of long read data in multi-sample lrRNA-seq experiments.

Netanya Keil[1,2], Carolina Monzó[4], Lauren McIntyre[1,2,3,*], Ana Conesa[4,*]

[1]Department of Molecular Genetics and Microbiology, University of Florida, Gainesville, FL, USA, 32610
[2]University of Florida Genetics Institute, University of Florida, Gainesville, FL, USA, 32610
[3] UF Health Cancer Center, University of Florida, Gainesville, FL, USA, 32610
[4]Institute for Integrative Systems Biology (I2SysBio), Spanish National Research Council (CSIC), Paterna, 46980, Spain

*corresponding authors: ana.conesa@csic.es; mcintyre@ufl.edu

ABSTRACT

SQANTI-reads leverages SQANTI3, a tool for the analysis of the quality of transcript models, to develop a read-level quality control framework for replicated long-read RNA-seq experiments. The number and distribution of reads, as well as the number and distribution of unique junction chains (transcript splicing patterns), in SQANTI3 structural categories are informative of raw data quality. Multi-sample visualizations of QC metrics are presented by experimental design factors to identify outliers. We introduce new metrics for 1) the identification of potentially under-annotated genes and putative novel transcripts and for 2) quantifying variation in junction donors and acceptors. We applied SQANTI-reads to two different datasets, a *Drosophila* developmental experiment and a multi-platform dataset from the LRGASP project and demonstrate that the tool effectively reveals the impact of read coverage on data quality, and readily identifies strong and weak splicing sites. SQANTI-reads is open source and available for download at GitHub.

INTRODUCTION

Short-read RNA sequencing (srRNA-seq) is the most common and cost-effective approach for studying the transcriptome. However, in srRNA-seq, transcripts must be inferred computationally, which can lead to inaccuracies in transcript identification (Liu et al. 2016; Newman et al. 2018). Recent advances in single-molecule long-read sequencing technologies have opened new avenues for transcriptome analysis (reviewed in (Marx 2023; van Dijk et al. 2023)). In long-read RNA sequencing (lrRNA-seq), full-length transcripts can be observed as single sequencing reads, allowing for direct transcript detection without the need for an assembly step. However, like any technology, lrRNA-seq is not without errors, and factors such as mRNA degradation, library preparation failures, and sequencing inacurracies can introduce biases into the data.

A database tracking bioinformatic tools for long-read sequencing (Amarasinghe et al. 2021) identifies numerous tools for the initial processing of lrRNA-seq data to assess the accuracy of base-calling and the length of the reads. These include pycoQC (Leger and Leonardi 2019), longQC (Fukasawa et al. 2020), nanoQC (De Coster et al. 2018), which offer a first-pass analysis of lrRNA-seq read quality. Other tools, such as SQANTI3 (Pardo-Palacios et al. 2024a), TALON (Wyman et al. 2020), FLAMES (Holmqvist et al. 2021), IsoSeq (https://isoseq.how/), and IsoTools (Lienhard et al. 2023), focus on evaluating transcript models inferred from the data. However, most current tools for lrRNA-seq read quality control were developed during the early stages of these technologies and are generally limited in the number of evaluated features and/or samples. As long-read sequencing technologies rapidly evolve, improving both in quality and experimental scope, the need for a comprehensive and comparative read quality assessment becomes increasingly critical.

Hence, the rapid decline in costs implies that the use of lrRNA-seq will continue to expand, with experimental designs involving multiple samples becoming more common (Glinos et al. 2022;

Joglekar et al. 2024; Mahmoud et al. 2024; Patowary et al. 2024)). From a quality control perspective, this necessitates that datasets are homogeneous, without biases associated with experimental groups, and free of outliers. Moreover, the generated data must be sufficient to address the research questions that motivated the experiment. The increase in throughput now makes it possible to design experiments that include barcoding and multiplexing to balance library preparation and sequencing across experimental groups (Auer and Doerge 2010). This approach helps avoid confounding technical variation with the treatments of interest and facilitates discriminating between failed technical replicates and failed samples. Finally, technological advancements such as more accurate basecallers (https://github.com/nanoporetech/dorado) and the availability of novel library preparation methods such as MAS-Iso-Seq (Al'Khafaji et al. 2024), CapTrap (Carbonell-Sala et al. 2024), R2C2 (Volden et al. 2018), Nano3P-seq (Begik et al. 2023) or FLAM-seq (Legnini et al. 2019) motivates the need for tools that can easily evaluate how these improvements impact various aspects of the long-read data quality.

In this context, we present SQANTI-reads, an extension of SQANTI3 (Pardo-Palacios et al. 2024a), a tool originally designed for transcript model quality control, to jointly provide quality control metrics for long-read data and to analyze multiple samples for consistency and bias. We demonstrate that SQANTI3's structural categories and other quality control metrics, repurposed in SQANTI-reads, are highly effective for assessing the homogeneity in a lrRNA-seq multi-sample experiment, identifying read quality control failures, and detecting outliers. Additionally, we have add new metrics that provide insights into the potential utility and discovery power of the data, including variation at donor/acceptor sites and identification of potentially under-annotated genes and mis-annotated transcripts. SQANTI-reads offers an extensive array of summary output tables, is customizable to accommodate any experimental design, and is available as an open-source, freely accessible tool.

RESULTS

SQANTI-reads can be used to evaluate long-read technology improvements

Long-read methods are rapidly improving and both Nanopore and PacBio are updating their instruments, kits and algorithms. Tools that can readily evaluate the broad impact on data quality of these technical improvements are highly needed to make informed decisions for downstream analyses. Our *Drosophila* dataset contained the same set of samples processed on the MinION and Promethion Instruments through several runs and analyzed with two base callers, the default Guppy and the new Dorado algorithm. A first question is whether Dorado effectively improved data quality without introducing biases and if data from several sequencing experiments could be merged. SQANTI-reads was used to address these questions. We first compared the Guppy and Dorado basecallers using SQANTI-reads metrics. As anticipated, Dorado resulted in more reads with assignable barcodes, a higher number of mapped reads, more reads aligning to annotated genes, more reads aligning to annotated transcripts, and more longer reads, without an increase in the proportion of reads with technical artifacts (Supplementary Figure 1, Supplementary file 2). This confirms that Dorado improves base-calling accuracy without introducing unwanted biases and motivated the selection of Dorado base-called reads for subsequent analyses.

In the *Drosophila* experiment, libraries were barcoded, pooled, and multiplexed across different MinION and PromethION runs, with a re-pooling step between the two machines. We used SQANTI-reads to compare the quality of the MinION and the PromethION runs, and to evaluate the consistency of the MinION and PromethION technology across technical replicates. The first MinION run (TR1) had higher percentages of reads with NIC/NNC and with non-canonical junctions compared to the second and third technical MinION runs (TR2, TR3) and compared to the PromethION runs for the same libraries (Supplementary Figure 2). MinION runs TR2 and TR3 were similar in their quality metrics (described below) to the PromethION run of the same samples, and the technical replicates on the PromethION were similar. These results indicate that the technology performs consistently across instruments and runs. Based on these SQANTI-reads QC results we aggregated data across technical replicates to further evaluate the quality of the

125 lrRNA-seq experiment. Although TR1 had lower quality than the other technical replicates, the
126 overall read numbers were low and we decided to keep this technical replicate in our evaluation
127 of the samples.
128
129 **SQANTI-reads metrics can be used to evaluate the global quality of the lrRNA-seq experiment**
130 In a multi-sample lrRNAseq experiment, all samples should be of similar quality. SQANTI3 uses
131 the FSM structural category to identify long-read sequences whose junctions are consistent with
132 an annotated transcript model. However, for a lrRNA-seq experiment to accurately reflect the
133 analyzed transcriptome, the reads should ideally also capture the distribution of transcript
134 lengths of the expressed transcriptome. The distribution of transcript lengths depends on the
135 species with *Drosophila* having overall less complex and shorter transcripts than human
136 (Supplementary Figure 3). A dataset with reads substantially shorter than the targeted
137 transcriptome but with still a high number of FSM indicates capture of short transcripts, while
138 combining shorter than expected reads with a high proportion of ISM may indicate RNA
139 degradation. We looked at these values for an initial assessment of the quality of the *Drosophila*
140 experiment.
141
142 First, we compared the number of reads and length distributions for all samples. The difference
143 in sequencing depth between the two developmental stages was evident, and motivated by the
144 the additional PromethION run on the 3-8 day samples (Figure 1A). For all samples, most reads
145 were shorter than 1kb with less than 20% of them above the 1 kb threshold (Figure 1B,
146 Supplementary Figure 4A). While between 53% and 67% of the reads across samples were
147 classified as FSM, 20% to 38% were labeled as ISM, and NIC/NNC were under 10% of the reads
148 (Figure 1C). For the reads greater than 1 kb, between 73% and 82% of the reads were FSM while
149 10% and 18% were ISM (Figure 1D). These results suggest that the *Drosophila* dataset contains a
150 significant proportion of short reads leading to incomplete transcript sequences.
151
152 To further understand how read quality affects gene and transcript quantification, we examined
153 these metrics aggregated by gene and UJC. We found that, despite the large sequencing depth

differences between developmental stages, the number of detected genes was only slightly lower in the 0-1 h samples (Figure 1E). However, these genes were quantified with fewer reads (80% genes with < 50 reads) than the 3-8 d samples, which had between 30% and 50% of genes with more than 100 reads (Figure 1E). Interestingly, when evaluating UJC we found that, while the number of UJC mirrored the sequencing depth pattern (Figure 1F), with 3-8 d samples showing five times more UJC than 1 h samples, and a larger number of FSM and ISM UJC, there were many additional UJC detected by fewer than 10 reads, and usually by a single read (Figure 1F & 1G) and these UJC were most frequently NIC/NNC (Supplementary Figure 4B & 4C). Downstream analyses would therefore need to address whether this represents novel low-expressed transcripts or technology errors. In contrast, the percentage of FSM reads between the two time points differed by less than 1x in all replicates (Figure 1H). These results indicate that the higher sequencing depth of the 3-8 d samples does not change the number of detected genes or annotated transcripts (FSM). The higher read depth per gene/ UJC suggests that more genes and transcripts will be able to be quantitatively evaluated in the 3-8 day samples compared to the 0-1 hour samples.

In the *Drosophila* data, we noticed two samples (RIL 12279 rep 1 0-1 hour red arrow; RIL 11255 3-8 day rep 3 - teal arrow) that had the lowest percentage of FSM and highest percentage of ISM in the 0-1 hour and 3-8 day groups respectively (Figure 1C). To determine whether these two samples were of overall lower quality than the rest, we examined their SQANTI-reads metrics. We found that RIL 12279 rep 1 had a lower proportion of FSM across all genes (Figure 1H) and a higher proportion of genes quantified with only one gene (Figure 1F), while RIL 11255 rep 3 had a similar gene (Figure 1H), UJC (Figure 1G) and % FSM in genes (Figure 1H) than other 3-8 day samples. We concluded that RIL 12279 rep 1 0-1 hour is a low-quality sample.

Altogether, this example shows that SQANTI-reads metrics can be used to compare samples and experimental conditions in a multi-sample experiment, detect outliers, and suggest points of attention for downstream data processing.

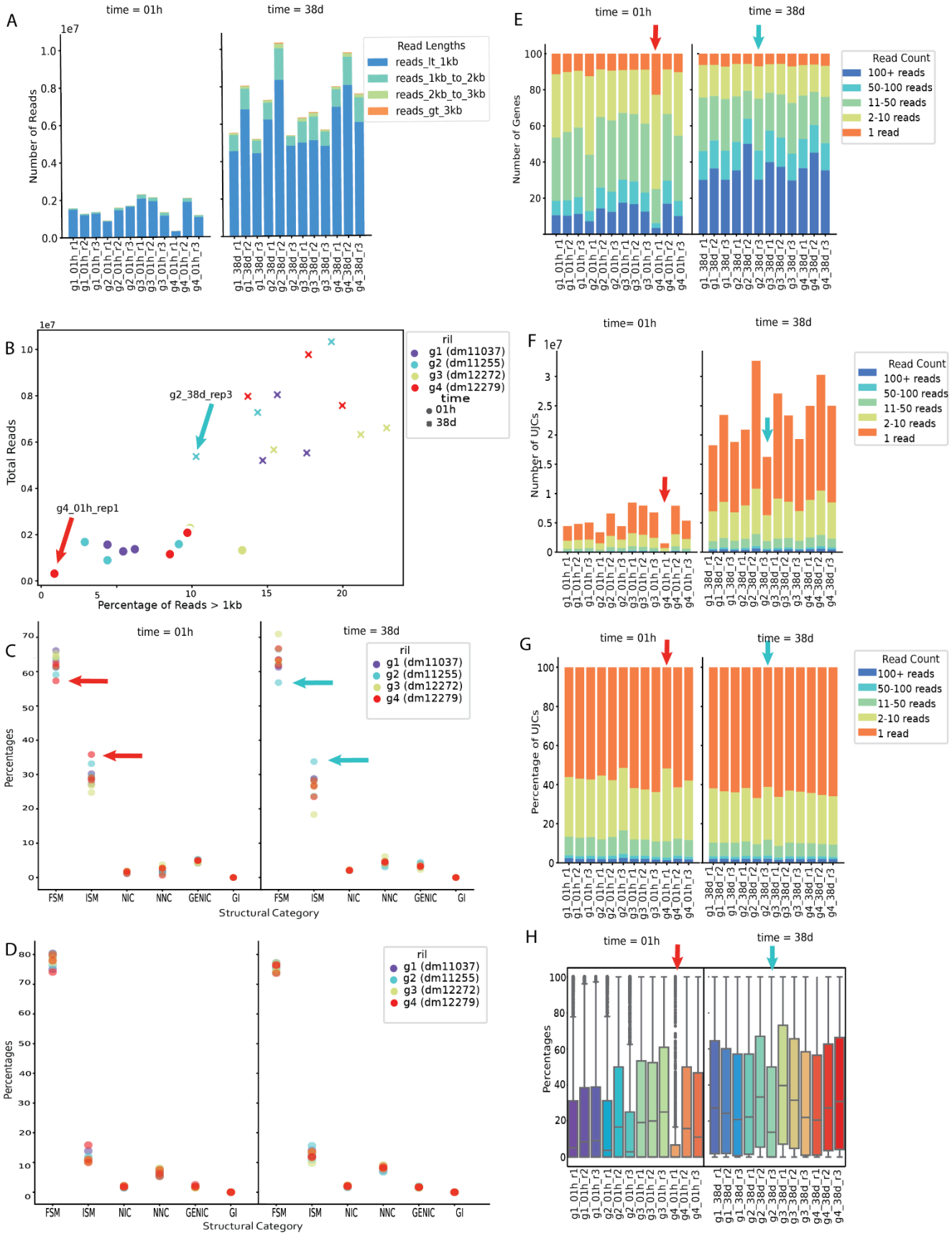
A
time = 01h
time = 38d
Number of Reads
Read Lengths
reads_lt_1kb
reads_1kb_to_2kb
reads_2kb_to_3kb
reads_gt_3kb
E
Number of Genes
Read Count
100+ reads
50-100 reads
11-50 reads
2-10 reads
1 read
B
Total Reads
Percentage of Reads > 1kb
g2_38d_rep3
g4_01h_rep1
ril
g1 (dm11037)
g2 (dm11255)
g3 (dm12272)
g4 (dm12279)
time
01h
38d
F
time= 01h
Number of UJCs
C
Percentages
Structural Category
FSM
ISM
NIC
NNC
GENIC
GI
G
Percentage of UJCs
D
H

Figure 1: SQANTI-reads analysis of *Drosophila* samples. A) Number of mapped reads by experimental group labeled with read length. B) Percentage of mapped reads >1kb vs percentage of reads that are FSM. Dots represent early stage (0-1 hours after enclosure) and crosses indicate adult stage (3 to 8 days old). The four genotypes are indicated with four different colors. C) Percentage of reads mapping to genes in each SQANTI3 structural category D) Percentage of reads mapping to genes in each SQANTI3-QC structural category for reads >1kb E) Number of genes detected with breakdown by the number of reads mapped to each gene. F) Number of UJCs detected with breakdown by the number of reads associated with each UJC. G) Proportion of UJCs detected with breakdown by the number of reads associated with each UJC. H) Distribution of the percentage of FSM reads by gene across samples.

SQANTI-reads metrics can be used to identify systematic differences among samples

The previous example demonstrated that SQANTI-reads metrics are effective in assessing dataset consistency. However, SQANTI-reads evaluates over 35 quality metrics, making it challenging to determine which features contribute to potential differences among samples. We include Principal Component Analysis (PCA) analysis to identify which metrics are the most relevant for quality variability when there are differences among samples or between groups. The percentage of reads and UJCs in each structural category, percentage of artifact reads (RT-switching, non-canonical junctions and intrapriming), percentage of junctions in each category, as well as length metrics, are included in the PCA.

We applied SQANTI-reads PCA analysis of quality features to investigate differences in read quality among various long-read sequencing methods used in the LRGASP challenge (Pardo-Palacios et al. 2024b), focusing on the WTC11 dataset. The analysis revealed that WTC11 samples clustered based on the long-read technology applied (Figure 2A). Specifically, PC1, which explains 56% of the variance, distinguished cDNA ONT samples from those generated by the other two technologies, while PC2, accounting for 35% of the variance, highlighted differences between dRNA ONT and cDNA PacBio. To further explore these differences, we examined the loadings for each principal component. Quality features with the highest positive loadings in PC1 included the number of reads, the percentage of reads and the proportion of UJCs in the NNC category, while features with high negative loadings included Intergenic and Genic Genomic reads. Several junction-related variables also exhibited high absolute loadings on PC1 (Figure 2B). SQANTI-reads plots confirmed these structural category differences between cDNA ONT samples and other library preparations. cDNA ONT had both the highest proportion of NNC reads and UJCs, (Figure

217 2C and 2D) and also had the lowest proportion of intergenic reads (Figure 2C). Other differences
218 in sequencing throughput and junction characteristics were also confirmed (Supplementary
219 Figure 5).
220
221 Upon examining the feature loadings for PC2, we found that variables with high contributions
222 included several metrics related to read length (Figure 2B). Consequently, we evaluated the
223 SQANTI-reads "Lengths of All Mapped Reads" plot for this experiment. Indeed, we observed that
224 the cDNA PacBio method produced a significantly higher proportion of reads between 1-2 kb, 2-
225 3 kb, and greater than 3 kb, as suggested by their negative loadings, compared to the dDNA ONT
226 method, which predominantly generated reads shorter than 1 kb (Figure 2E). Similarly,
227 percentage of reads assigned as ISM with high positive values was higher in dRNA ONT samples
228 (Figure 2 C).
229
230 In conclusion, we showed that the SQANTI-reads PCA analysis is an effective tool for uncovering
231 significant read quality differences between long-read sequencing methods and for revealing
232 unexpected technology biases.
233

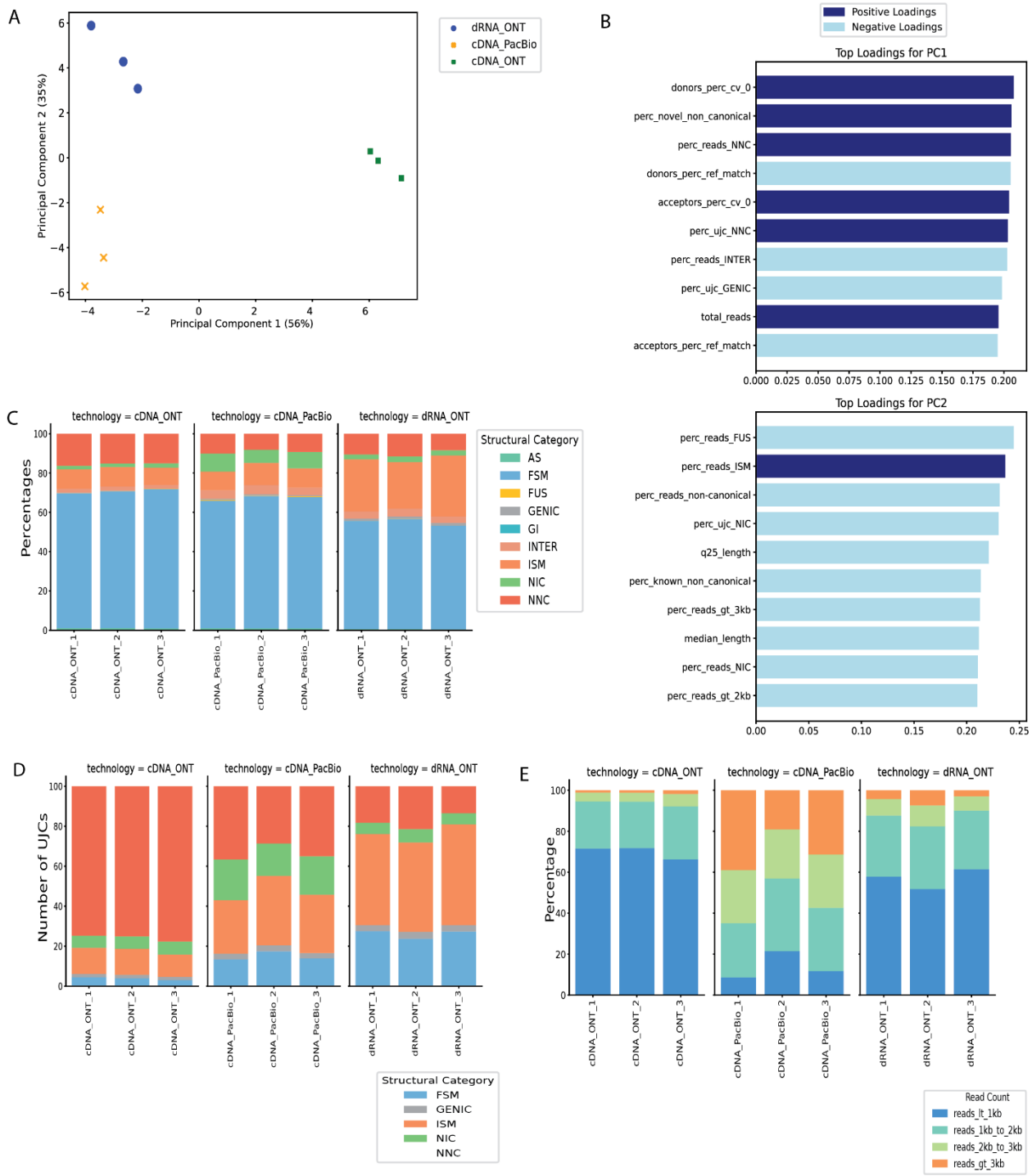

Figure 2: SQANTI-reads PCA analysis of LRGASP WTC11 samples A) PCA using SQANTI-reads quality features. B) Top 10 Loadings for PC1 and PC2. C) Distribution of reads in SQANTI structural categories. D) Distribution of UJCs in structural categories E) Distribution of read lengths for all mapped reads.

243 **SQANTI-reads identifies potentially under annotated genes.**

244 Long-read data often reveal a large number of sequences that cannot be exactly matched to
245 existing annotations. In many cases, these UJC belong to annotated genes and are identified by
246 only a few reads, as illustrated by the SQANTI-reads analysis in Figures 1 and 2. This suggests they
247 could be either low-expressed transcripts or technological artifacts. However, in some instances,
248 a high proportion of reads in a gene may correspond to the same novel UJC, indicating the
249 possibility of a previously unannotated transcript that warrants closer examination. SQANTI-
250 reads includes a customizable decision tree to identify such cases (see Methods, Figure 3A).
251 Basically, the tool identifies genes with a high (R > threshold) number of reads, with novel UJC
252 containing a large fraction (Q > threshold) of the gene´s splice sites and capturing a high
253 proportion (P > threshold) of the reads. We applied this approach to the WTC11 PacBio data
254 using default parameters (R=100, P=20 and Q=80). The logic for defining expressed genes as well
255 annotated or underannotated is described in Figure 3A. The annotation category for all expressed
256 genes (default: number of reads in gene (R) > 100) are provided in the gene_classification.csv file.
257 From the set of expressed genes, we identified 8,556 well annotated genes, 88% of which have a
258 well covered annotated transcript (>20% of total gene coverage) (Figure 3B). We also identified
259 101 genes, for which there are no reads with an FSM match to an annotated transcript. Of these
260 54% have a well covered UJC. For all expressed genes with well covered unannotated UJC, we
261 identified 424 that contained most of the observed junctions in that gene (>80%), and we label
262 these putative novel transcripts (Figure 3C). Of these, 316 were NIC and 108 were NNC. The
263 SQANTI-reads output for putative novel transcripts is included in the
264 putative_underannotation.csv file (Table 2).

265

266 For genes with at least one putative novel transcript (R>100, P>20, Q>80) and an annotated
267 transcript (FSM) we selected the FSM with the highest proportion of reads. We then compared
268 the structure of the putative novel transcripts to the most expressed annotated transcript using
269 TranD (Nanni et al. 2024). For genes with an annotated transcript that is relatively highly
270 expressed (>20% of the reads for that gene), 103 putative candidate transcripts differed from the
271 annotated transcript by donor/acceptor variation, suggesting a possible alternative splice site. In

addition, 10 putative candidate transcripts had an extra exon; 15 a skipped exon and 9 with both missing and skipped exons relative to the most expressed annotated UJC (Figure 3D). For the genes where the annotated transcript represented less than 20% of the reads in that gene, the putative novel transcript differed from the annotated transcript by an alternative exon in 147 cases (33 extra exons, 86 skipped exons, and 43 with both an extra and skipped exon) (Figure 3E). Details and scripts for this analysis are provided in the Supplementary Methods.

This analysis shows that SQANTI-reads can readily identify under-annotated genes and flag putative novel transcript models that contain interpretable alternative exonic patterns that deserve further attention.

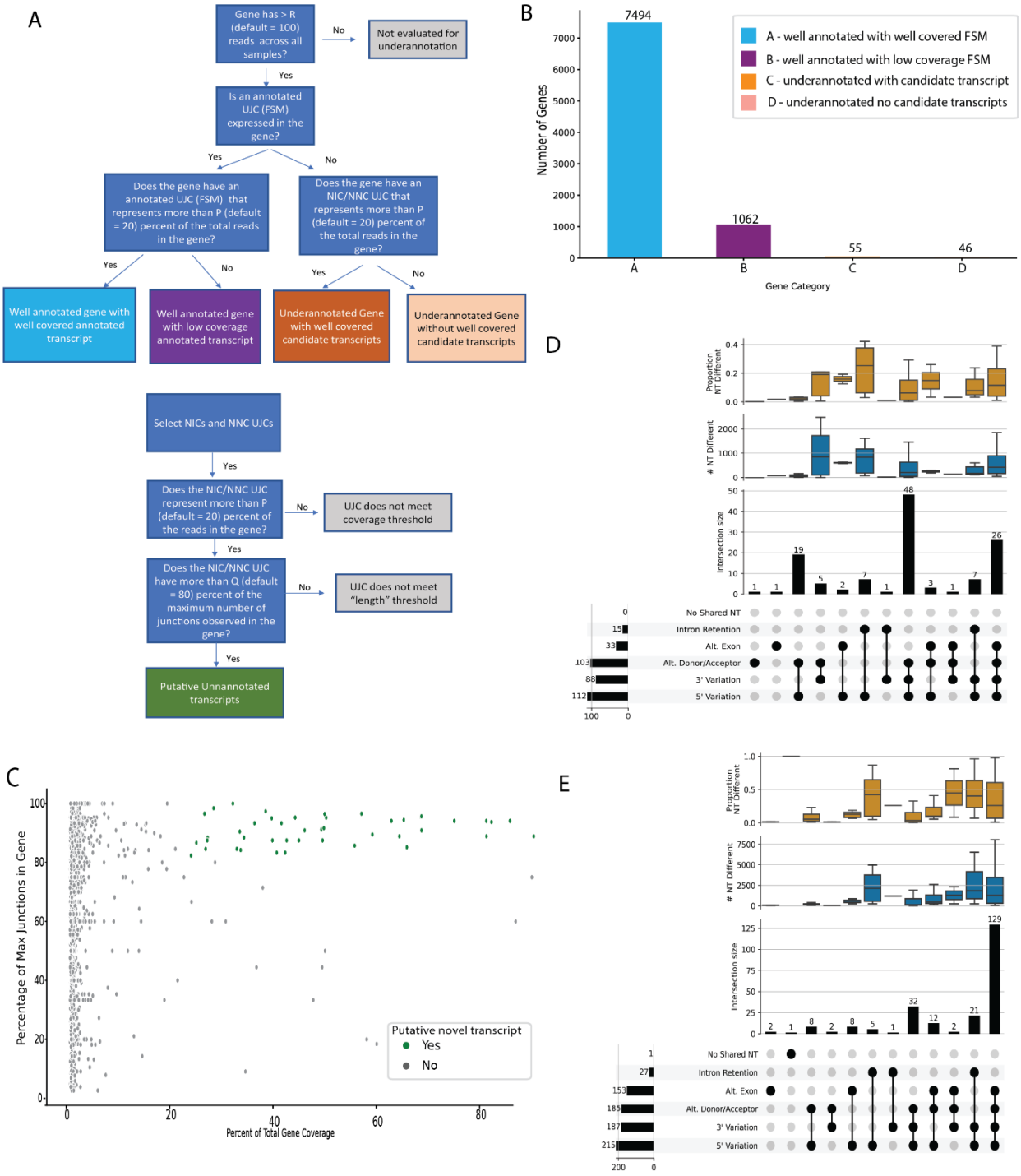

Figure 3: Evaluation of WTC11 PacBio samples for under-annotated genes. A) Decision tree for classifying genes as well annotated or under-annotated and classifying transcripts as putative novel candidate transcripts. B) Number of genes by their annotation status according to SQANTI-reads parameters. C) The coverage (percent of total reads) vs length (percentage of maximum junctions) for all UJCs in underannotated genes with well covered candidate transcripts. UJCs that meet the thresholds for putative novel transcripts are colored in green. D&E) Comparison of putative candidate novel transcripts with the most expressed annotated

transcript in that gene for well-annotated genes with well-covered FSMs (D) and with an FSM detected but without < 20% of the total reads in the gene(E).

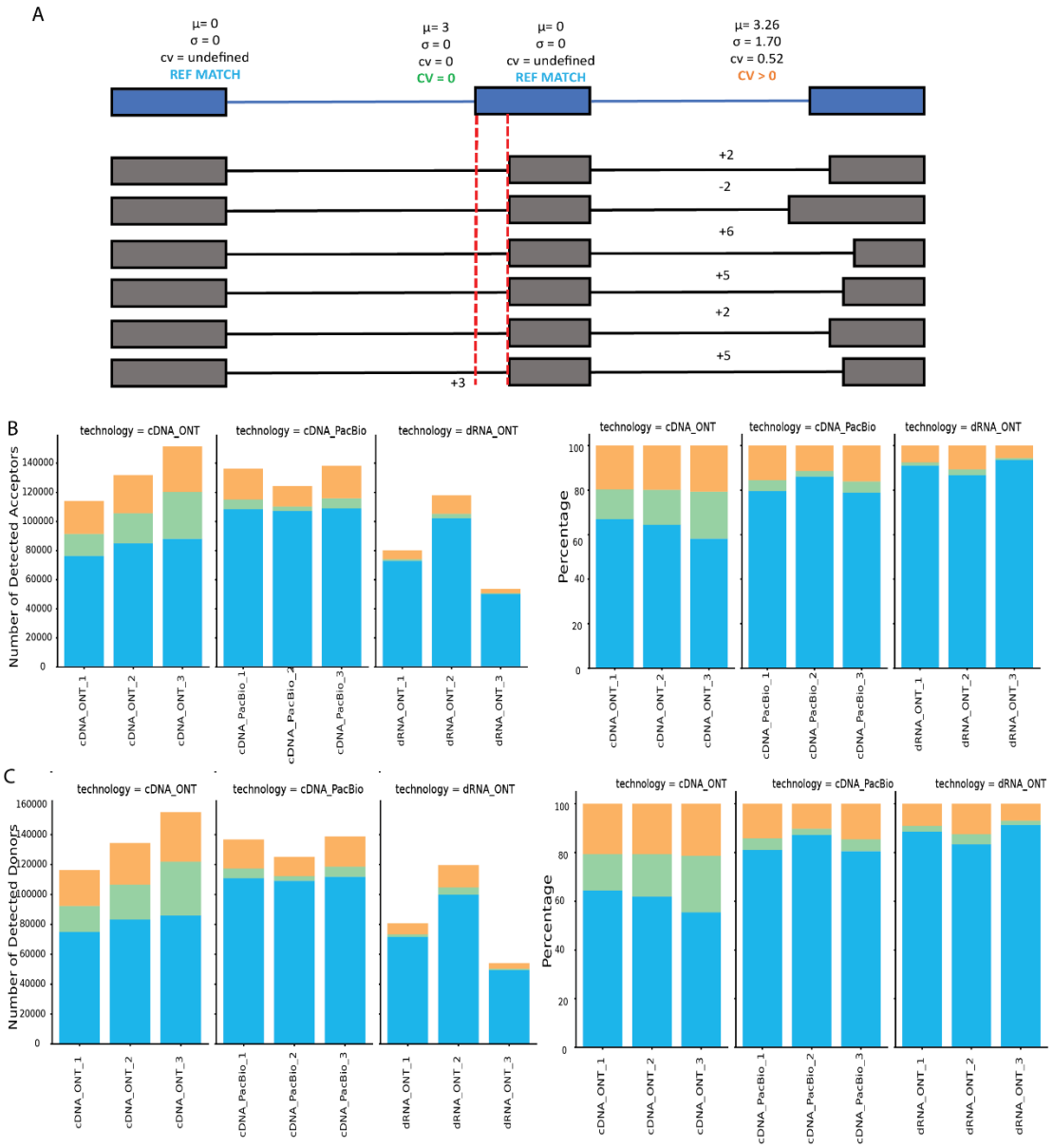

Figure 4. Variation in donors/acceptors. Metrics are only calculated for annotated donor/acceptors with a minimum threshold of reads (10 by default). A) Metrics for the classification of donor/acceptor variation. When all reads align to the annotated donor/acceptor this is classified as a reference match (Ref Match). When all reads align to the same donor/acceptor location, but this is not the annotated position this is classified as CV = 0. When reads align in multiple positions in proximity to an annotated donor/acceptor this is classified as CV > 0. B) Classification of the number (left) and proportion (right) of detected acceptors faceted by technology. C) Classification of the number (left) and proportion (right) of detected donors faceted by technology.

304 **SQANTI-reads metrics for donors/acceptors identify noisy splicing and potentially novel splice-**
305 **sites**
306 SQANTI-reads calculates the mean, standard deviation and coefficient of variation (CV) for all
307 expressed annotated donors/acceptors (Figure 4A). A value CV > 0 indicates variability in the
308 donor/acceptor, with higher CV values indicating more variability. Variability around a splice-
309 junction may be due to weak splicing (Wang and Marín 2006) or to technology errors and
310 mapping accuracy, for example due to junction ambiguity (Li 2018). We evaluated these metrics
311 on the WTC11 dataset for reference junctions with at least 10 reads. We found similar patterns
312 in the variability (CV > 0) in donors and acceptors (Figure 4B). All three technologies identify
313 donors and acceptors with variability around the splice site (CV > 0). Donors/acceptors with CV >
314 0 consistently across the three technologies, are highly suspicious of 'noisy' splicing or a weak
315 splice site and may be worth follow up (Supplementary Figure 6A and 6B). The SQANTI-reads
316 output file cv.csv identifies the donors/acceptors with CV > 0 making it straightforward to follow
317 up on particular locations with tools such as Integrative Genomics Viewer (IGV) (Robinson et al.
318 2011).
319
320 A reference match junction indicates that the splice signal is strong (Wang and Marín 2006; Dent
321 et al. 2021). Results for cDNA PacBio and dRNA-seq were similar, with both showing a higher
322 number and proportion of reference match donors/acceptors compared to cDNA ONT (Figure 4B
323 and C) despite these technologies detecting similar numbers of FSM UJCs (Figure 2D). We
324 compared the FSM UJCs identified by the three methods (Supplementary Figure 7A). Most of the
325 FSM UJCs were detected by all three technologies (n = 19690), with a similar number detected
326 by cDNA PacBio only (n = 8110) and cDNA ONT (n = 9360) only. We hypothesized that the
327 difference in the number of reference match donors/acceptors was potentially due to longer
328 transcripts with more junctions being detected in cDNA PacBio compared to shorter transcripts
329 with fewer junctions in dRNA ONT and cDNA ONT. For the FSMs detected only in one technology
330 we plotted the distribution of the number of junctions and confirmed that the cDNA PacBio FSM
331 transcripts had a larger number of junctions compared to dRNA ONT and cDNA ONT

332 (Supplementary Figure 8). This agrees with cDNA PacBio showing longer reads than both ONT
333 technologies in the WTC11 dataset (Figure 2E).
334
335 Splice junctions may differ from annotated sites due to the presence of novel donors/acceptors.
336 The category CV = 0 identifies donor/acceptors with no variability but differing from the
337 annotated donor/acceptor, representing strong candidates for *bona fide* alternative splice sites.
338 We evaluated the donors and acceptors with CV = 0 in all the technologies (Supplementary Figure
339 6E and 6F). We identified 51 donors and 34 acceptors with CV=0 in all three technologies. Of
340 these, 76% of donors and 65% of acceptors are within 12nt of an annotated donor/acceptor
341 indicating a potential mis-annotation of the splice-site (Supplementary Figure 9). These donors
342 and acceptors with CV = 0 across all technologies were detected by a minimum of 10 reads and
343 in some cases could be detected with > 100 reads (Supplementary Figure 10). Supplementary
344 Figure 11 shows an example of one of the reference donors with CV = 0 detected across all 3
345 technologies. This donor is in the H2AZ1 gene at position 99,948,814 on chromosome 4. All the
346 reads associated with this donor map to position 99,948,811 which is 3 nts away from the
347 annotated donor position (Supplementary Figure 11). Donors and acceptors with CV = 0 detected
348 consistently across samples and/or technologies indicate potential robust detection of
349 alternative splice sites.
350
351
352 **DISCUSSION**
353
354 The increase in throughput and generalization of lrRNA-seq has led to the growing popularity of
355 experiments containing many samples. Multiple lrRNA-seq studies of lrRNA-seq have shown that,
356 despite technological improvements, biases associated with read length and accuracy are still
357 present in lrRNA-seq data (Amarasinghe et al. 2020; Delahaye and Nicolas 2021). These biases
358 vary between the major LRS platforms and with the introduction of new instruments and
359 chemistries. Other types of systematic biases, such as those introduced by batches utilized in
360 large experiments, may also occur. Benchmarking studies have also revealed that transcript
361 reconstruction methods can yield highly different results due to the varying strategies used to

362 resolve data inaccuracies (Pardo-Palacios et al., 2024b). This highlights the need for tools that
363 can comprehensively evaluate the characteristics of raw long-read data before making decisions
364 on downstream analyses. Direct examination of read quality enables the researcher to evaluate
365 the experiment for consistency and identify any outlier samples and any systematic differences
366 in read quality between sample groups. We have developed SQANTI-reads as a tool that enables
367 a comprehensive assessment of reads obtained from a LRS experiment. We leverage the widely
368 adopted SQANTI3-QC framework and we add several metrics designed specifically for the
369 assessment of reads to provide an effective strategy for evaluating the quality of lrRNA-seq multi-
370 sample experiments. Mapped reads are summarized by their inferred junctions, start and end
371 positions and using SQANTI3 categories and sub-categories each read is classified. A summary of
372 all the observed patterns of junctions, and the distance between annotated and observed donors
373 and acceptors are tallied by sample. If meta-data is included in the design file, sample groupings
374 can be used to compare SQANTI-classifications and junction metrics. Alternate groupings based
375 on different columns in the meta-data are enabled without needing to rebuild the classification
376 and junction files.
377
378 For example, in Oxford Nanopore Technology (ONT) the existence of multiple platforms at
379 different price points for different numbers of pores (Flongle, MinION, GridION, PromethION)
380 but with the same library protocols means that in a large experiment, samples can be initially
381 evaluated at low cost on one of the lower throughput platforms (Flongle MinION) and if samples
382 are of sufficient quality, then can be run on higher throughput platforms (GridION, PromethION).
383 Sample multiplexing and running on multiple 'lanes' is good experimental design practice (Auer
384 and Doerge 2010). Our SQANTI-reads analysis of the Drosphila dataset illustrates such scenario.
385 In this case the pool for the 0-1 hour samples was initially evaluated on the MinION. The resulting
386 data from TR1 were unbalanced and had relatively short reads with a high proportion of ISM.
387 These observations enabled adjustment of the library concentrations and run parameters, and a
388 second minion run resulted in fewer ISM and more balance in read numbers across libraries. A
389 PromethION run based on the rebalanced libraries efficiently used the sequencing resources
390 across samples. The same procedure was deployed with the 3-8 day samples, and while

391 rebalancing helped ensure efficiency of the subsequent two PromethION runs. This example
392 illustrates both good experimental design practices for large experiments and the utility of
393 SQANTI-reads in assessing data quality at early stages of data acquisition, enabling corrections
394 that lead to a successful sequencing experiment.
395
396 Another important aspect of lrRNA-seq multi-sample experiments is the ability to quickly assess
397 whether the data can address the biological questions that motivated the study. This includes,
398 among other things, whether genes and transcripts are sufficiently quantified and if potential
399 novel transcripts are adequately supported. While these questions may ultimately be answered
400 after full data processing with transcript reconstruction algorithms, users may find it helpful to
401 evaluate support directly from the raw data.
402
403 SQANTI-reads provides information on the distribution of reads across genes and UJC (a raw-data
404 proxy for transcripts) and introduces new metrics for identifying variations in donors/acceptors,
405 under-annotated genes, and putative novel transcripts for further evaluation. These metrics
406 enable the researcher to quickly determine if more reads are needed, and whether there are
407 highly expressed putative novel transcripts potentially worth detailed experimentation.
408
409 The examples presented in this work demonstrate that SQANTI-reads is flexible and
410 customizable, allowing users to explore the impact of various experimental design factors on
411 read, UJC, and donor/acceptor properties, as well as identifying potential novel transcripts. The
412 output from SQANTI-reads can be easily mined for additional insights and used to direct attention
413 and resources toward interesting and novel features of lrRNA-seq experiments. We expect
414 SQANTI-reads to become an essential tool for the QC of multi-sample lrRNA-seq datasets.
415

416 ## METHODS

417 **SQANTI-reads basics**

418 SQANTI-reads is an adaptation of SQANTI3 designed to evaluate individual reads rather than
419 transcript models. It allows for the comparison of multiple samples, providing quality control

results across the entire experiment. Several new features have been introduced to address the specific needs of QC in multi-sample experiments, while some functionalities of SQANTI3 have been removed as they are not applicable to read-level processing. Table 1 highlights the major differences between SQANTI3 and SQANTI-reads, emphasizing the new features of SQANTI-reads, while Table 2 lists the names and descriptions of the output files.

Table 1. Comparison between SQANTI3 and SQANTI-reads

Feature	**SQANTI3**	**SQANTI-reads**
Sequences analyzed	transcript models	reads
Annotation with SQANTI3 categories	yes, for transcript models	yes, for reads and UJCs
Computation of SQANTI3 quality metrics	yes	yes
Samples processed	One	Multiple
Visualizations across samples	no	yes
PCA analysis between samples	no	yes
Summary of read counts (per gene, per UJC)	no	yes
Donor/acceptor variation metrics	no	yes
Identification of putative under annotated genes	no	yes
Identification of putative novel transcripts	no	yes
Machine learning validation of transcript models	yes	no
IsoAnnot annotation	yes	no

Table 2. SQANTI-reads specific output files

Output file	**Description**	**Default output**	**Output type**
gene_counts.csv	Number of reads in each structural category, per gene and per sample	Yes	Multiple samples file
ujc_counts.csv	List of junction hashes in each sample and the number of reads in	Yes	Multiple samples file

	each sample associated with each junction string. Flags the most expressed UJC per gene		
length_summary.csv	Number and percentage of reads in length categories per sample	Yes	Multiple samples file
cv.csv	Metrics on the coefficient of variance of reference junctions for each sample	Yes	Multiple samples file
jxn_counts.csv	Number of known canonical, novel canonical, known non-canonical, and novel non-canonical junctions in reads of each sample	- - all-tables	Multiple samples file
cv_acc_counts.csv cv_don_counts.csv	Number of detected annotated donors and acceptors in each junction variation category	- - all-tables	Multiple samples file
FSM_counts.csv ISM_counts.csv NIC_NNC_counts.csv	Number of reads in each subcategory for FSMs, ISMs, NICs, and NNCs	- - all-tables	Multiple samples file
err_counts.csv	Number and percentage of reads with evidence of intrapriming, RT-switching, and non-canonical junctions per samples	- - all-tables	Multiple samples file
pca_loadings.csv	PC1 and PC2 loadings from PCA	–pca-tables	Summary file
pca_variance.csv	Variance explained by each PC	–pca-tables	Summary file
gene_classification.csv	For genes with coverage over a user-defined threshold, gives the annotation category of each gene	Yes	Summary file
putative_underannotation.csv	Metrics on NIC and NNC UJCs and flags putative novel transcripts	Yes	Summary file

The input files for SQANTI-reads include: 1) a GTF file of read alignments, 2) a reference genome FASTA file, 3) a GTF file of the reference transcript model annotation, and 4) a design file containing metadata for multiple samples. The first step of SQANTI-reads involves using the SQANTI3-QC module to generate SQANTI3-like classification and junction files, with the classification file containing one row for each mapped read. Reads are classified according to the SQANTI categories (Tardaguila et al. 2018) as full-splice match (FSM), incomplete-splice match

437 (ISM), novel-in-catalog (NIC), novel-not-in-catalog (NNC), antisense, fusion, genic genomic, and
438 intergenic. SQANTI3 subcategories are also included, based on 5' and 3' end positions relative to
439 the annotated transcription start sites (TSS) and transcription termination sites (TTS) (Pardo-
440 Palacios et al. 2024a). Additionally, the reverse transcriptase (RT) switching algorithm of
441 SQANTI3-QC identifies reads with evidence of RT switching events, while reads with more than
442 60% adenines in the 20 bp downstream of the reported TTS at the genomic level are flagged as
443 potential intrapriming events. The length of each read and the number of exons in each read are
444 also recorded in the classification file.
445
446 **Junction Metrics**
447 The SQANTI-reads junction file follows the same format as the SQANTI3 junction file, with each
448 row representing a junction in a read, including the start and end positions of the junction. The
449 distance from the junction start and end to the nearest annotated junction start and end in the
450 reference GTF is calculated. It's important to note that the nearest annotated start and end
451 positions may not belong to the same annotated junction. SQANTI classifies junctions as known
452 or novel, and as canonical or non-canonical, based on the dinucleotide pairs at the junction's start
453 and end. By default, dinucleotide combinations of GT-AG, GC-AG, and AT-AC are considered
454 canonical, while any other combinations are classified as non-canonical, although the user can
455 specify additional canonical sites.
456 SQANTI-reads introduces new metrics to evaluate the relationship between the junctions in
457 mapped reads and the annotated donors and acceptors. In the SQANTI3-QC junction file, the
458 distance from each donor/acceptor in each read to the nearest annotated donor/acceptor is
459 recorded. In SQANTI-reads, the mean absolute distance in nucleotides from the annotated
460 donor/acceptor site, the standard deviation, and the coefficient of variation (CV = standard
461 deviation/mean) are calculated and included in the cv.csv file. Each detected junction is classified
462 as 1) Reference Match junction if the mean distance and the standard deviation to an annotated
463 junction are both equal to 0; 2) CV = 0 junction when the mean distance is greater than 0 and the
464 standard deviation equals 0, and 3) CV > 0 junction when the CV is greater than 0.
465

466 **Unique Junction Chain and gene-level information**

467 SQANTI-reads groups mapped reads based on their full junction pattern and refer them to as
468 Unique Junction Chains (UJCs). Each UJC is labeled with a string that includes the chromosome
469 and junction coordinates (Nanni et al. 2024). To enhance computational efficiency, UJC strings
470 are encoded as an index in a hash table (JxnHash). The read count for each JxnHash is calculated
471 and included in the ujc_counts.csv file. Additionally, the number of known canonical, known non-
472 canonical, novel canonical, and novel non-canonical junctions within each UJC is annotated, along
473 with the SQANTI structural category of the UJC. The number of reads within each structural
474 category for each gene, as well as the total number of reads per gene, is stored in the summary
475 file gene_counts.csv.

476

477 **Identifying genes that may be under-annotated and transcripts that may be mis-annotated**

478 For expressed genes, a high proportion of reads from a UJC classified as NIC/NNC may indicate
479 the presence of a potentially novel transcript. SQANTI-reads includes a customizable pipeline to
480 identify genes with such potential under-annotation events. The procedure identifies NIC/NNC
481 UJCs that meet a minimum number (R) and proportion (P) of reads, with default values set at 100
482 reads and 20%, respectively. To mitigate the risk that the NIC/NNC UJC is merely a degradation
483 product, an additional condition is applied: the candidate UJC must include at least 80% of the
484 gene's junctions (Q) (Figure 3A). The R, P, and Q thresholds are pipeline parameters that can be
485 adjusted by the user. Furthermore, SQANTI-reads allows for the evaluation of under-annotated
486 genes and novel transcripts within a specific subset of samples associated with a particular
487 experimental factor (e.g., developmental stage or technology) using the --factor-level option.

488

489 **Multi-sample processing**

490 SQANTI-reads processes multiple samples to generate classification and junction files when a
491 design file (Supplementary file 1) is provided to the sqanti-reads.py command. If individual
492 samples have already been pre-processed with SQANTI3-QC, SQANTI-reads can be run in --fast
493 mode, where the design file links the individual classification and junction files to sample IDs for
494 the calculation of SQANTI-reads metrics, summaries, and a series of visualizations. If pre-

495 processing has not been done, SQANTI-reads is run in --simple mode where SQANTI3 is run on
496 each sample, followed by the calculation of SQANTI3 metrics and summaries. The output also
497 includes a summary for each sample, reporting the mean, median, upper quartile, and lower
498 quartile of mapped read length, as well as the number and proportion of reads that are shorter
499 than 1 kb, between 1 and 2 kb, between 2 and 3 kb, and greater than 3 kb in length, all of which
500 are included in the length_summary.csv file.
501
502 ***Drosophila melanogaster* data**
503 A total of 24 samples corresponding to 2 developmental stages (0-1 hours and 3-8 hours post-
504 hatching) and four genotypes (dmel 11037, 11255, 12272 and 12279) (3 samples per
505 experimental condition) were sequenced using Oxford Nanopore Technology (ONT). One
506 barcoded cDNA library was built per sample, the 12 samples from the 0-1 hour and the 12
507 samples from the 3-8 day stages were pooled and sequenced on a MinION. Data were evaluated
508 with PycoQC (Leger and Leonardi 2019) which focuses on read length and base quality. All
509 samples passed this basic QC, libraries were re-pooled and run on the PromethION. Detailed
510 metadata for these samples are provided in Supplementary Table 1. Raw electrical data were
511 processed with the default Guppy basecaller. Samples were stored in .fast5 format and as .fastq
512 files. The .fast5 files were converted to the Dorado compatible .pod5 format using pod5 (v 0.3.6)
513 and then processed in Dorado (v 0.5.2) (https://github.com/nanoporetech/dorado) using options
514 --recursive --device "cuda:0,1" --kit-name SQK-PCB109 --trim none. Reads were demultiplexed
515 using the demux mode of Dorado (v 0.5.2) with options --no-classify --emit-fastq resulting in
516 separate Dorado fastq files for each sample. The fastq files generated by Guppy/Dorado were
517 both processed using pychopper (v 2.7.1), the oriented fastq files were aligned to *D.*
518 *melanogaster* 6.50 and the resulting sam files were converted to gtf using samtools (v 1.10) (Li et
519 al. 2009) and bedtools (v 2.29.2) (Quinlan and Hall 2010). The resulting gtf files (67 technical
520 replicates from 24 samples), the *D. melanogaster* 6.50 fasta reference file
521 (https://ftp.flybase.net/releases/FB2023_01/dmel_r6.50/ (Öztürk-Çolak et al. 2024)), and a
522 design file (Supplementary File 2) were used as input to SQANTI-reads. The *Drosophila* dataset
523 includes, therefore, two experimental conditions (time and genotype) and two technical
524 conditions (sequencing platform and base caller) with the experimental samples multiplexed and

525 evaluated with both technical conditions. The SQANTI-reads output for this dataset is provided
526 in Supplementary File 3.
527
528 **Human Cell line WTC11**
529 We used publicly available lrRNA-seq data from the Long-read RNA-seq Genome Annotation
530 Assessment Project (Pardo-Palacios et al. 2024b) to illustrate the utility of SQANTI-reads.
531 Specifically, we used triplicate measurements of the transcriptome of the WTC11 human cell line
532 that were profiled by cDNA PacBio Sequel II, cDNA Oxford Nanopore Minion, and direct RNA
533 Oxford Nanopore Minion methods. Data were downloaded from the ENCODE website
534 (https://www.encodeproject.org/search/?type=Experiment&internal_tags=LRGASP). Accession
535 numbers for these samples are provided in Supplementary Table 2. The fastq files were pre-
536 processed by LRGASP researchers as described in (Pardo-Palacios et al. 2024b). We used the gtf
537 files of read alignments, GENCODE's GRCh38.p13 reference genome gtf and fasta for release 38
538 (https://www.gencodegenes.org/human/release_38.html), and a design file (Supplementary file
539 4) to run SQANTI-reads on the WTC11 samples. The SQANTI-reads output is provided in
540 Supplementary File 5.
541
542 **Acknowledgements**
543 This work was supported in part by a grant from the National Institutes of Health
544 (1R21HG011280-01), the Spanish MICIN (PID2020-119537RB-I00), the European Union's
545 programme Horizon Europe under the Marie Skłodowska-Curie Actions postdoctoral fellowship
546 to C.M. (101149931). This work is also supported in part by a grant from the National Cancer
547 Institute (NCI P01 CA214091), the National Institute of General Medical Sciences (NIGMS
548 GM137430), the University of Florida Department of Molecular Genetics and Microbiology, the
549 University of Florida Genetics Institute, the University of Florida Cancer Center, and the
550 University of Florida Research Computing Center (www.rc.ufl.edu) and the Latin American and
551 Caribbean Scholars award to N.K. Part of the computations were performed on the high
552 performance computing cluster Garnatxa at the Institute for Integrative Systems Biology
553 (I2SysBio). I2SysBio is a joint research center formed by University of Valencia (UV) and Spanish

National Research Council (CSIC). We acknowledge Ashley Myrick for help with some of the initial CV plots and Knife Bankole for the initial coding of the junction hash. Alison Morse prepared all samples and libraries for the *Drosophila* experiment, ran all initial QC analyses and recalled all the bases for ONT data. We acknowledge Rolf Renne for his support.

Competing interest statement

A.C. has received in-kind funding from Pacific Biosciences for library preparation and sequencing. A.C. collaborates with Oxford Nanopore in the Marie Skłodowska-Curie Actions Doctoral Network project LongTREC (Grant Agreement # 101072892).

Author contributions

N.K. conducted research, developed software implementations, created figures and drafted manuscript. C.M. revised code, integrated new methods into SQANTI Github and helped with data analysis. L.M. conceived and supervised the study and drafted the manuscript. A.C. supervised the study, contributed to conceptualizations and drafted the manuscript.

Data access

Drosophila long read data are available at the sequencing read archive (SRA) under the Bioproject PRJNA1134728.

References

Al'Khafaji AM, Smith JT, Garimella KV, Babadi M, Popic V, Sade-Feldman M, Gatzen M, Sarkizova S, Schwartz MA, Blaum EM et al. 2024. High-throughput RNA isoform sequencing using programmed cDNA concatenation. *Nature Biotechnology* **42**: 582-586.

Amarasinghe SL, Ritchie ME, Gouil Q. 2021. long-read-tools.org: an interactive catalogue of analysis methods for long-read sequencing data. *GigaScience* **10**.

Amarasinghe SL, Su S, Dong XY, Zappia L, Ritchie ME, Gouil Q. 2020. Opportunities and challenges in long-read sequencing data analysis. *Genome Biology* **21**.

Auer PL, Doerge RW. 2010. Statistical Design and Analysis of RNA Sequencing Data. *Genetics* **185**: 405-416.

Begik O, Diensthuber G, Liu H, Delgado-Tejedor A, Kontur C, Niazi AM, Valen E, Giraldez AJ, Beaudoin JD, Mattick JS et al. 2023. Nano3P-seq: transcriptome-wide analysis of gene expression and tail dynamics using end-capture nanopore cDNA sequencing. *Nat Methods* **20**: 75-85.

588 Carbonell-Sala S, Perteghella T, Lagarde J, Nishiyori H, Palumbo E, Arnan C, Takahashi H,
589 Carninci P, Uszczynska-Ratajczak B, Guigó R. 2024. CapTrap-seq: a platform-agnostic and
590 quantitative approach for high-fidelity full-length RNA sequencing. *Nature*
591 *Communications* **15**: 5278.
592 De Coster W, D'hert S, Schultz DT, Cruts M, Van Broeckhoven C. 2018. NanoPack: visualizing
593 and processing long-read sequencing data. *Bioinformatics* **34**: 2666-2669.
594 Delahaye C, Nicolas J. 2021. Sequencing DNA with nanopores: Troubles and biases. *PloS one* **16**:
595 e0257521.
596 Dent CI, Singh S, Mukherjee S, Mishra S, Sarwade RD, Shamaya N, Loo KP, Harrison P,
597 Sureshkumar S, Powell D et al. 2021. Quantifying splice-site usage: a simple yet powerful
598 approach to analyze splicing. *NAR Genomics and Bioinformatics* **3**.
599 Fukasawa Y, Ermini L, Wang H, Carty K, Cheung MS. 2020. LongQC: A Quality Control Tool for
600 Third Generation Sequencing Long Read Data. *G3 (Bethesda)* **10**: 1193-1196.
601 Glinos DA, Garborcauskas G, Hoffman P, Ehsan N, Jiang L, Gokden A, Dai X, Aguet F, Brown KL,
602 Garimella K et al. 2022. Transcriptome variation in human tissues revealed by long-read
603 sequencing. *Nature* **608**: 353-359.
604 Holmqvist I, Bäckerholm A, Tian Y, Xie G, Thorell K, Tang KW. 2021. FLAME: long-read
605 bioinformatics tool for comprehensive spliceome characterization. *Rna* **27**: 1127-1139.
606 Joglekar A, Hu W, Zhang B, Narykov O, Diekhans M, Marrocco J, Balacco J, Ndhlovu LC, Milner
607 TA, Fedrigo O et al. 2024. Single-cell long-read sequencing-based mapping reveals
608 specialized splicing patterns in developing and adult mouse and human brain. *Nature*
609 *Neuroscience* **27**: 1051-1063.
610 Leger A, Leonardi T. 2019. pycoQC, interactive quality control for Oxford Nanopore Sequencing.
611 *Journal of Open Source Software* **4**: 1236.
612 Legnini I, Alles J, Karaiskos N, Ayoub S, Rajewsky N. 2019. FLAM-seq: full-length mRNA
613 sequencing reveals principles of poly(A) tail length control. *Nature Methods* **16**: 879-
614 886.
615 Li H. 2018. Minimap2: pairwise alignment for nucleotide sequences. *Bioinformatics* **34**: 3094-
616 3100.
617 Li H, Handsaker B, Wysoker A, Fennell T, Ruan J, Homer N, Marth G, Abecasis G, Durbin R. 2009.
618 The Sequence Alignment/Map format and SAMtools. *Bioinformatics* **25**: 2078-2079.
619 Lienhard M, van den Beucken T, Timmermann B, Hochradel M, Börno S, Caiment F, Vingron M,
620 Herwig R. 2023. IsoTools: a flexible workflow for long-read transcriptome sequencing
621 analysis. *Bioinformatics* **39**.
622 Liu P, Sanalkumar R, Bresnick EH, Keleş S, Dewey CN. 2016. Integrative analysis with ChIP-seq
623 advances the limits of transcript quantification from RNA-seq. *Genome Res* **26**: 1124-
624 1133.
625 Mahmoud M, Huang Y, Garimella K, Audano PA, Wan W, Prasad N, Handsaker RE, Hall S,
626 Pionzio A, Schatz MC et al. 2024. Utility of long-read sequencing for All of Us. *Nature*
627 *Communications* **15**: 837.
628 Marx V. 2023. Method of the year: long-read sequencing. *Nature Methods* **20**: 6-11.
629 Nanni A, Titus-McQuillan J, Bankole KS, Pardo-Palacios F, Signor S, Vlaho S, Moskalenko O,
630 Morse Alison M, Rogers RL, Conesa A et al. 2024. Nucleotide-level distance metrics to
631 quantify alternative splicing implemented in TranD. *Nucleic Acids Research* **52**: e28-e28.

632 Newman JRB, Concannon P, Tardaguila M, Conesa A, McIntyre LM. 2018. Event Analysis: Using
633 Transcript Events To Improve Estimates of Abundance in RNA-seq Data. *G3*
634 *Genes|Genomes|Genetics* **8**: 2923-2940.
635 Öztürk-Çolak A, Marygold SJ, Antonazzo G, Attrill H, Goutte-Gattat D, Jenkins VK, Matthews BB,
636 Millburn G, dos Santos G, Tabone CJ et al. 2024. FlyBase: updates to the Drosophila
637 genes and genomes database. *Genetics* **227**.
638 Pardo-Palacios FJ, Arzalluz-Luque A, Kondratova L, Salguero P, Mestre-Tomás J, Amorín R,
639 Estevan-Morió E, Liu T, Nanni A, McIntyre L et al. 2024a. SQANTI3: curation of long-read
640 transcriptomes for accurate identification of known and novel isoforms. *Nature*
641 *Methods* **21**: 793-797.
642 Pardo-Palacios FJ, Wang D, Reese F, Diekhans M, Carbonell-Sala S, Williams B, Loveland JE, De
643 María M, Adams MS, Balderrama-Gutierrez G et al. 2024b. Systematic assessment of
644 long-read RNA-seq methods for transcript identification and quantification. *Nature*
645 *Methods* **21**: 1349-1363.
646 Patowary A, Zhang P, Jops C, Vuong CK, Ge X, Hou K, Kim M, Gong N, Margolis M, Vo D et al.
647 2024. Developmental isoform diversity in the human neocortex informs
648 neuropsychiatric risk mechanisms. *Science* **384**: eadh7688.
649 Quinlan AR, Hall IM. 2010. BEDTools: a flexible suite of utilities for comparing genomic features.
650 *Bioinformatics* **26**: 841-842.
651 Robinson JT, Thorvaldsdóttir H, Winckler W, Guttman M, Lander ES, Getz G, Mesirov JP. 2011.
652 Integrative genomics viewer. *Nat Biotechnol* **29**: 24-26.
653 Tardaguila M, de la Fuente L, Marti C, Pereira C, Pardo-Palacios FJ, Del Risco H, Ferrell M,
654 Mellado M, Macchietto M, Verheggen K et al. 2018. SQANTI: extensive characterization
655 of long-read transcript sequences for quality control in full-length transcriptome
656 identification and quantification. *Genome Res* **28**: 396-411.
657 van Dijk EL, Naquin D, Gorrichon K, Jaszczyszyn Y, Ouazahrou R, Thermes C, Hernandez C. 2023.
658 Genomics in the long-read sequencing era. *Trends in Genetics* **39**: 649-671.
659 Volden R, Palmer T, Byrne A, Cole C, Schmitz RJ, Green RE, Vollmers C. 2018. Improving
660 nanopore read accuracy with the R2C2 method enables the sequencing of highly
661 multiplexed full-length single-cell cDNA. *Proceedings of the National Academy of*
662 *Sciences* **115**: 9726-9731.
663 Wang M, Marín A. 2006. Characterization and prediction of alternative splice sites. *Gene* **366**:
664 219-227.
665 Wyman D, Balderrama-Gutierrez G, Reese F, Jiang S, Rahmanian S, Forner S, Matheos D, Zeng
666 W, Williams B, Trout D et al. 2020. A technology-agnostic long-read analysis pipeline for
667 transcriptome discovery and quantification. *bioRxiv* doi:10.1101/672931: 672931.
668

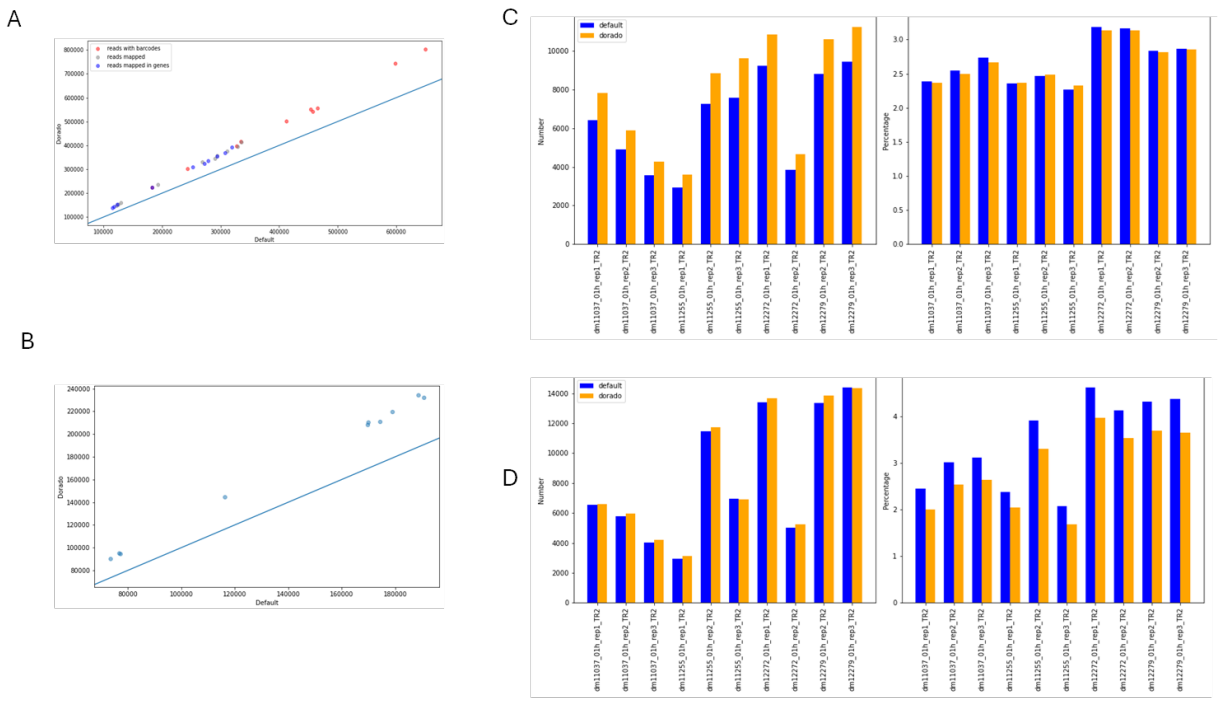

Supplementary Figure 1: Comparison of Guppy and Dorado basecalling for technical replicate 2. A) Number of reads with assignable barcodes (red), number of mapped reads (grey) and number of reads mapped in genes (blue) in Dorado vs Guppy. B) Number of reads >2kb in Dorado vs Guppy C) Number and percentage of reads with evidence of intrapriming in Dorado and Guppy D) Number and percentage of reads with non-canonical junctions in Dorado and Guppy.

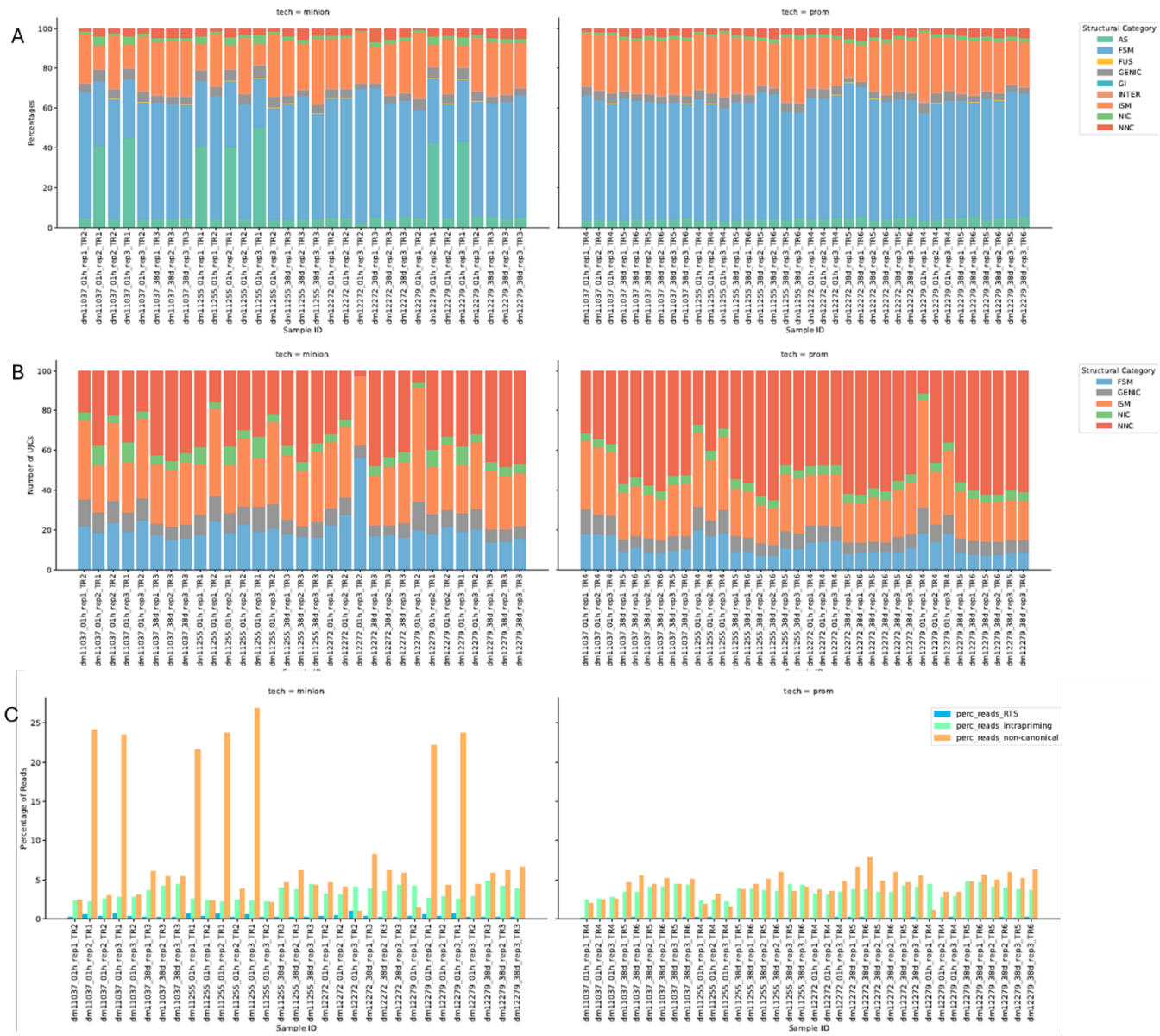

Supplementary Figure 2: *Drosophila* technical replicates basecalled with Dorado. A) Proportion of reads in each structural category. B) Proportion of unique junction chains (UJCs) in each structural category. C) Proportion of reads with evidence of RT-switching (blue), intrapriming (green) and non-canonical junctions (orange)

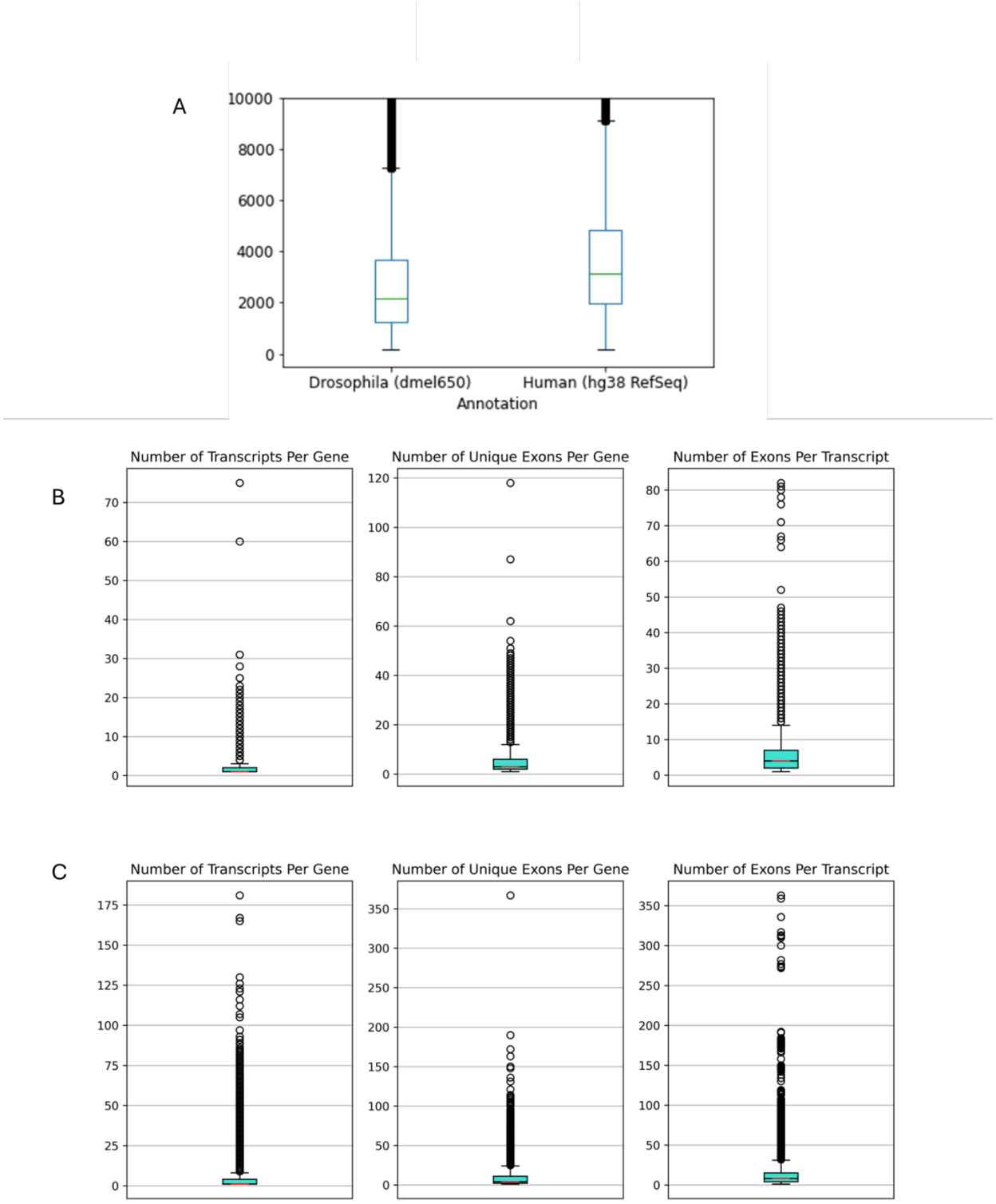

Supplementary Figure 3: Complexity Metrics of Drosophila (dmel650) and Human (hg38 Refseq) Annotations. A) Distribution of protein-coding transcript lengths in dmel650 and hg38 Refseq. B) Transcriptome Complexity Metrics for dmel650 C) Transcriptome complexity metrics for hg38 Refseq

A

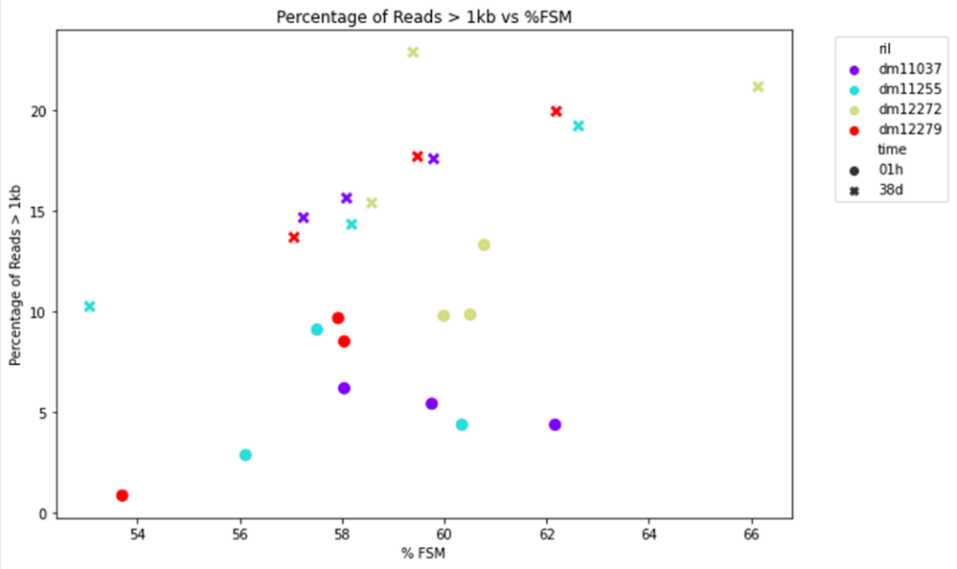
Percentage of Reads > 1kb vs %FSM
Percentage of Reads > 1kb
% FSM
ril
dm11037
dm11255
dm12272
dm12279
time
01h
38d

B

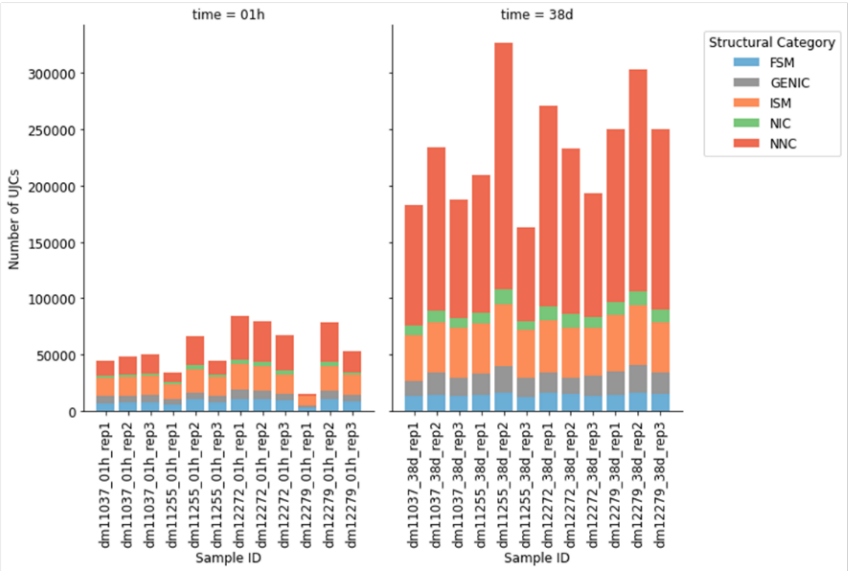
time = 01h
time = 38d
Number of UJCs
Sample ID
Structural Category
FSM
GENIC
ISM
NIC
NNC

C

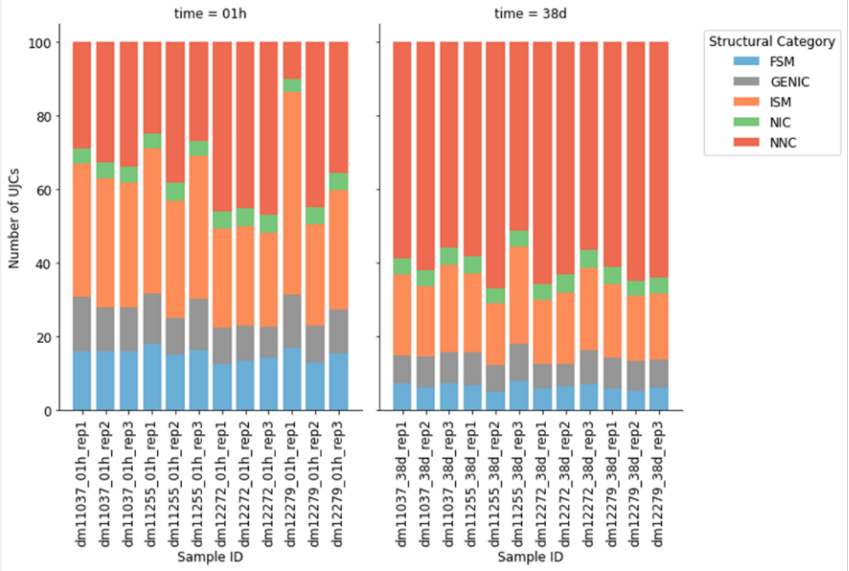
time = 01h
time = 38d
Number of UJCs
Sample ID
Structural Category
FSM
GENIC
ISM
NIC
NNC

Supplementary Figure 4: SQANTI-reads plots for *Drosophila* samples basecalled with Dorado A) Percentage of reads greater than 1kb vs Percentage of reads classified as full-splice match (FSM) B) Number of UJCs detected coloured by structural category of the UJC. C) Proportion of UJCs coloured by structural category of the UJC

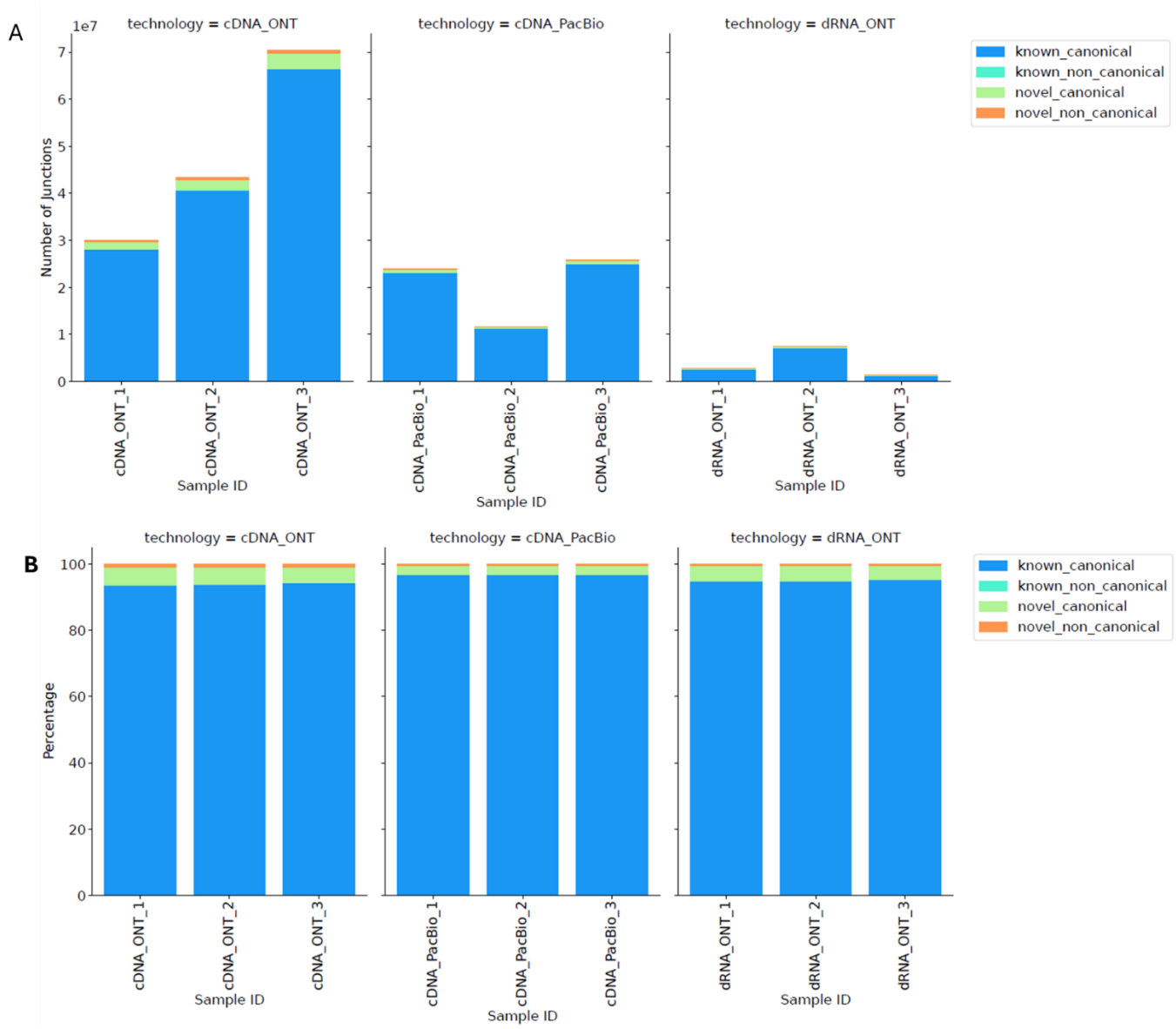

Supplementary Figure 5: Junction plots for WTC11 samples A) Number of junctions in reads coloured by junction categories (known-canonical, known-non-canonical, novel-canonical and novel-non-canonical) B) Proportion of junctions in reads in each junction category

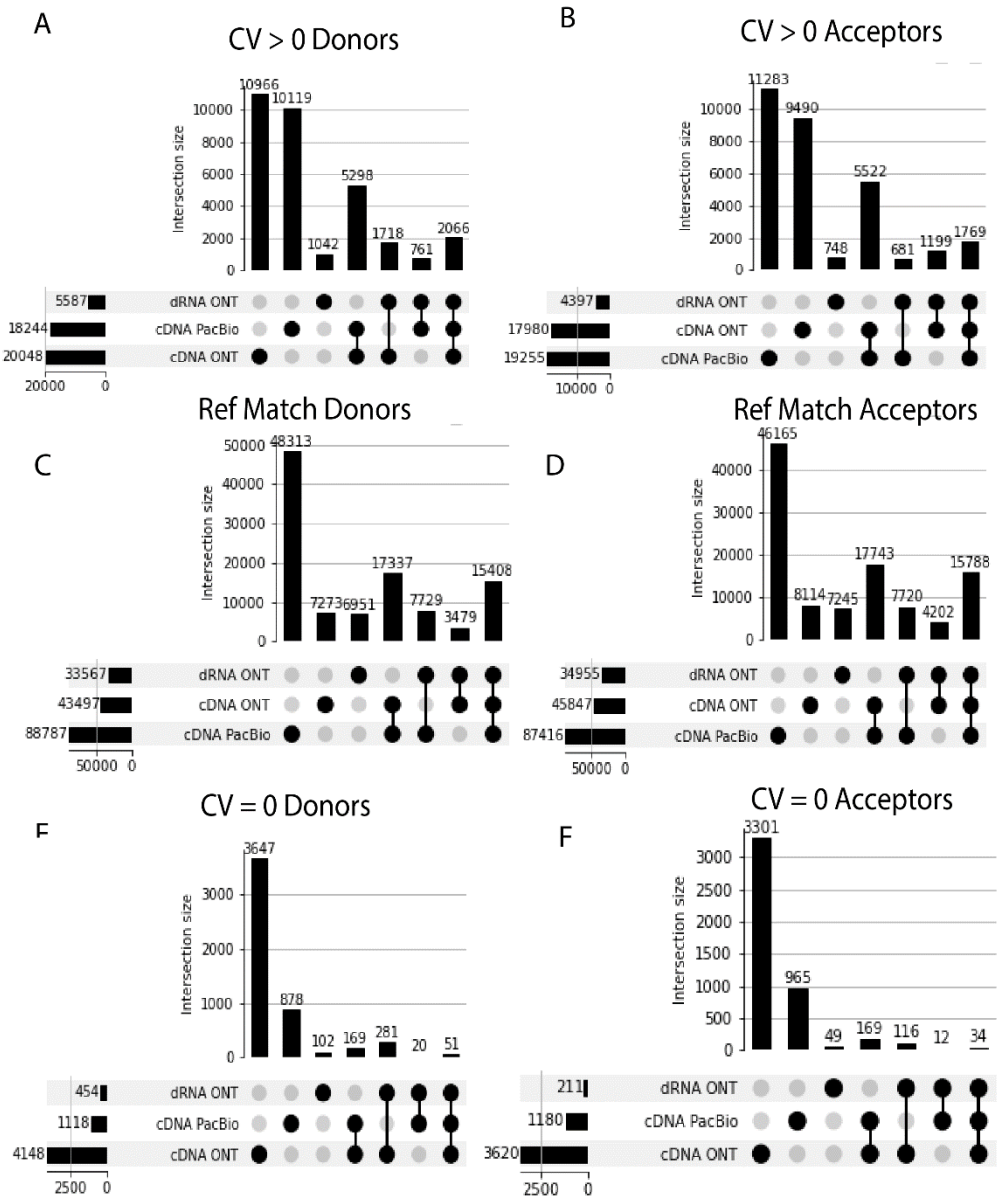

Supplementary Figure 6: Upset plot of donors and acceptors detected in replicate 1 of the WTC11 samples of each technology by variation category. CV > 0 donors (A) and acceptors (B) . Reference match donors (C) and acceptors (D). CV = 0 donors (E) and acceptors (F)

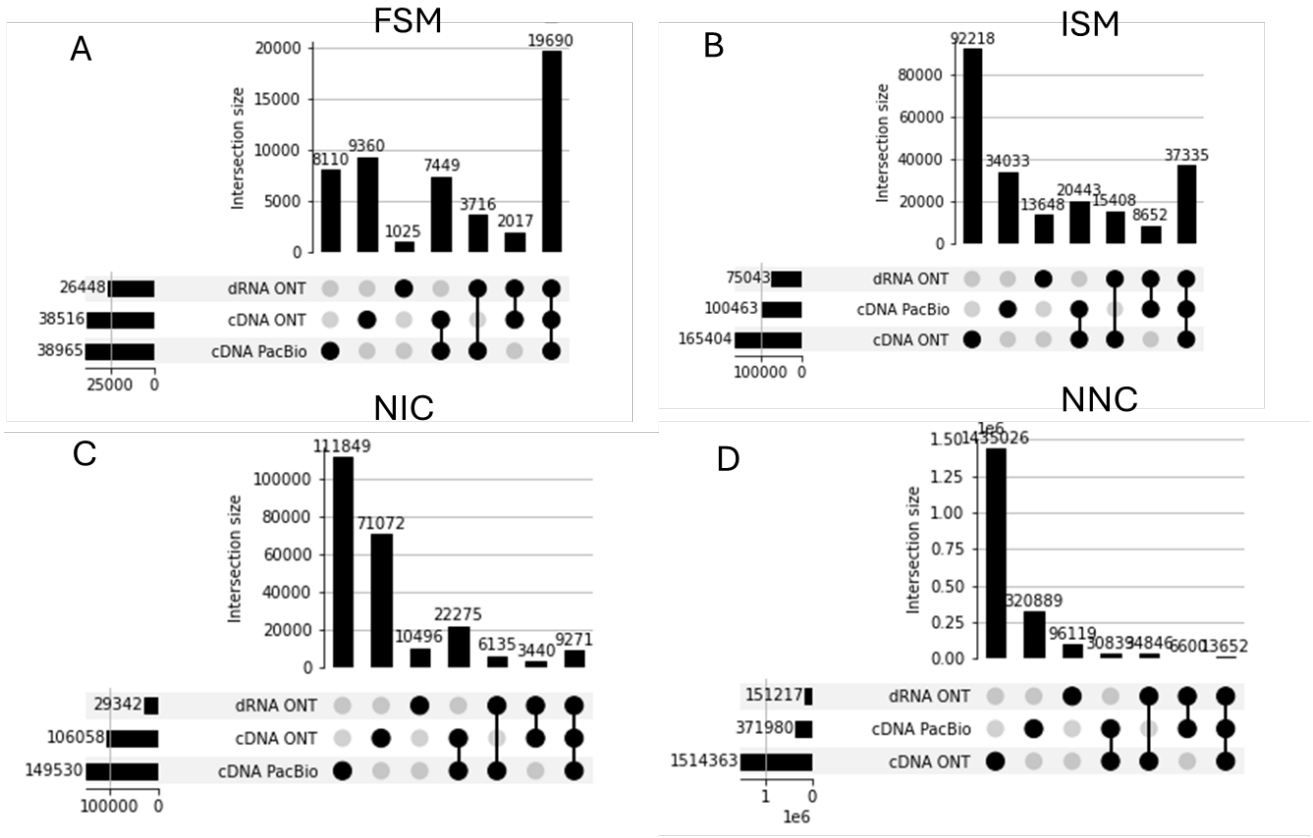

Supplementary Figure 7: Upset plot of multi-exon UJCs detected in each technology by structural category in the WTC11 samples. A) FSM UJCs B) ISM UJCs C) NIC UJCs and D) NNC UJCs

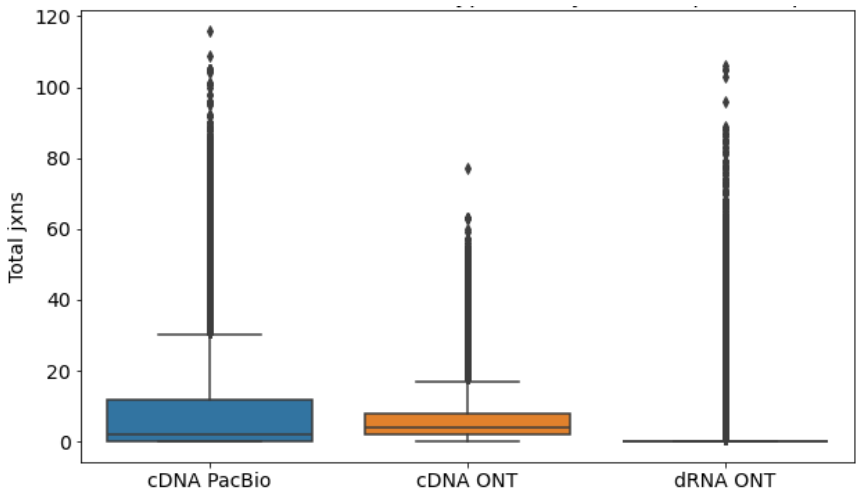

Supplementary Figure 8: Distribution of number of junctions in FSM UJCs detected exclusively in one technology for the WTC11 samples

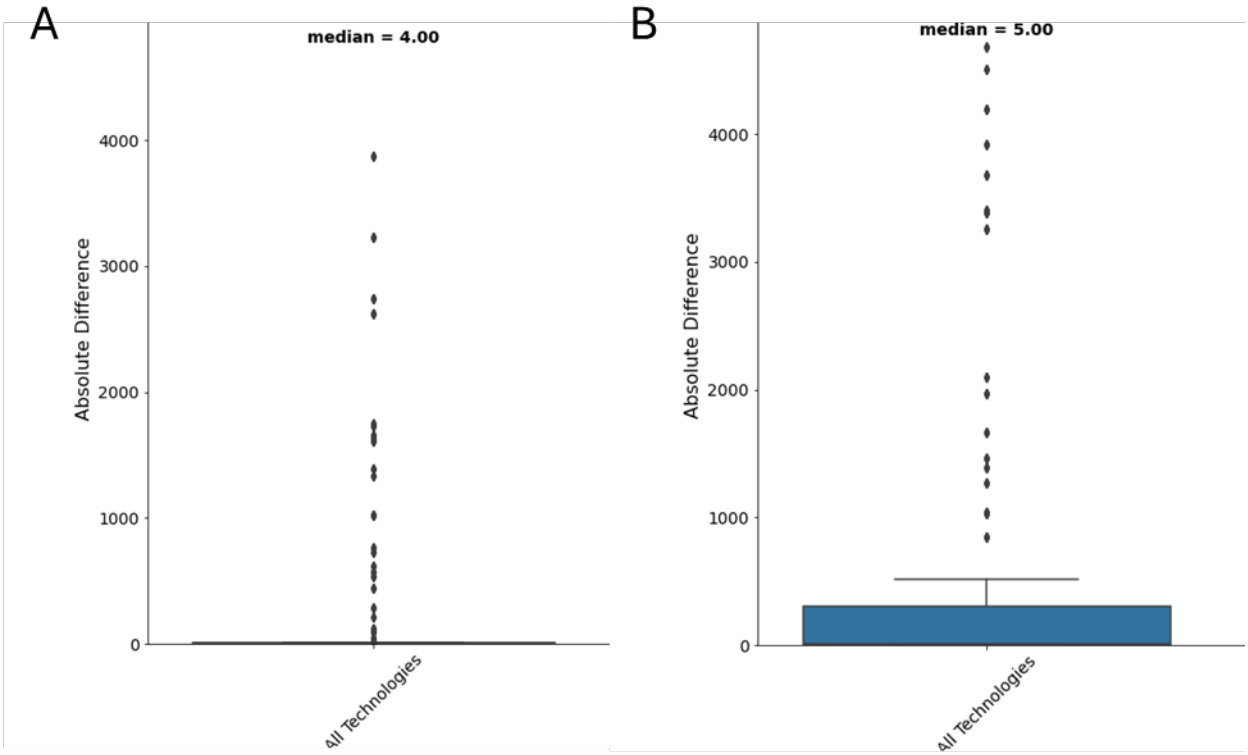

Supplementary Figure 9: For donors (A) and acceptors (B) with cv=0 in replicate 1 of the WTC11 samples, boxplot of the distribution of the distance of the read donors and acceptors to the annotated donors and acceptors in replicate 1.

A

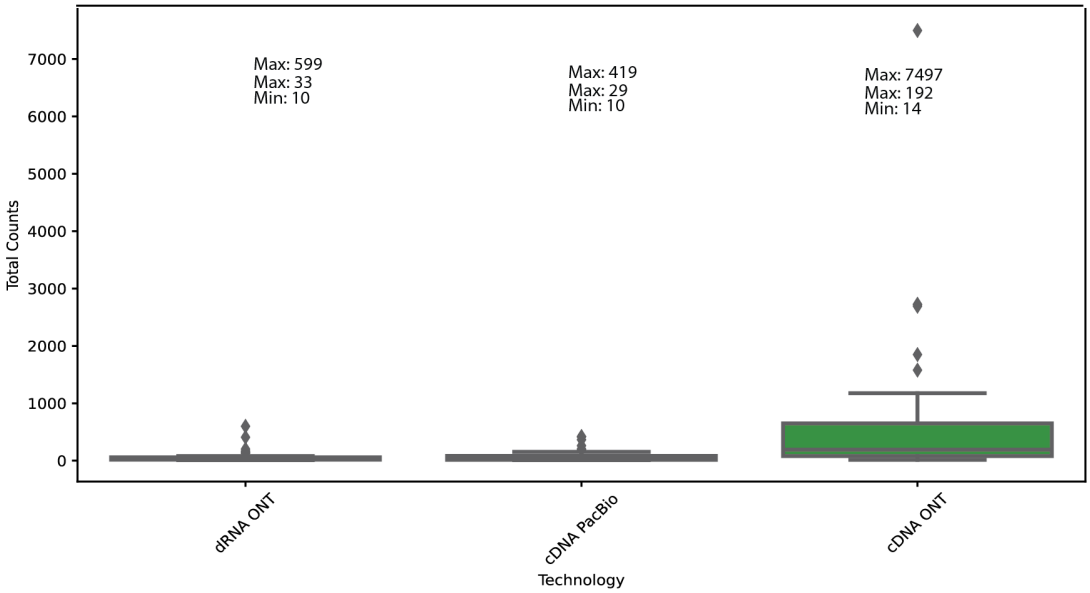

B

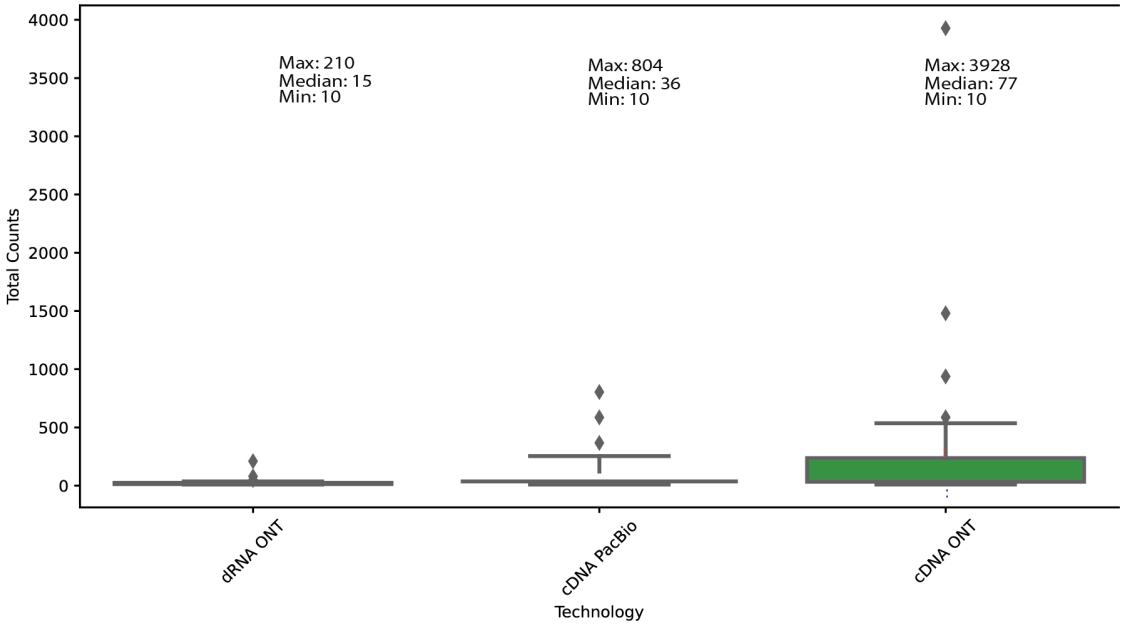

Supplementary Figure 10: For donors (A) and acceptors (B) with cv=0 in replicate 1 of the WTC11 samples, boxplot of the number of reads associated with the reference junction with cv=0.

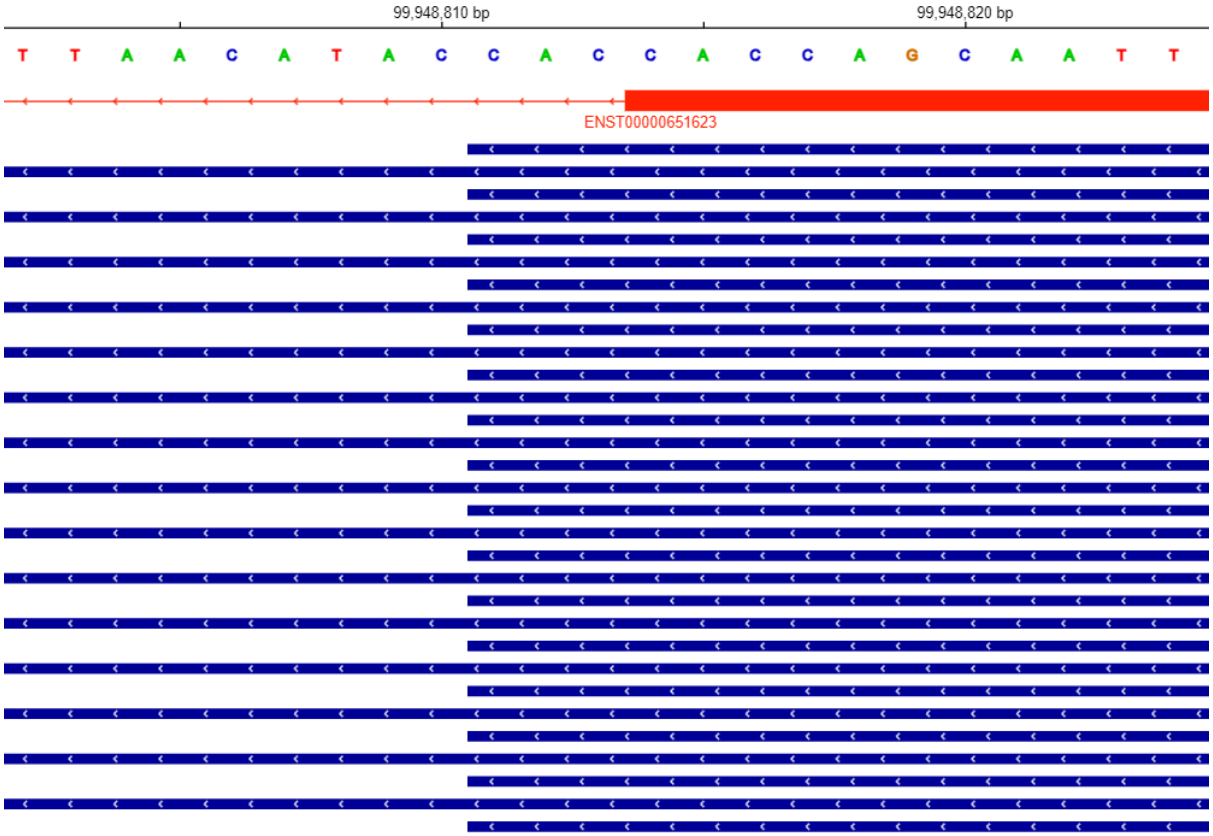

Supplementary Figure 11: IGV visualization of a reference donor with CV = 0 in the H2AZ1 gene at position 99,948,814 on chromosome 4. All of the reads associated with this donor map to position 99,948,811 which is 3 nts away from the annotated donor position. The annotated transcript is shown in red and the reads are shown in blue.

Supplementary Table 1: Metadata for Drosophila Experiment

Sample	Genotype	Stage	Number of Technical Replicates	Minion Runs	Promethion Runs
dm11037_01h_rep1	11037	01h	2	1	1
dm11037_01h_rep2	11037	01h	3	2	1
dm11037_01h_rep3	11037	01h	3	2	1
dm11255_01h_rep1	11255	01h	3	2	1
dm11255_01h_rep2	11255	01h	3	2	1
dm11255_01h_rep3	11255	01h	3	2	1
dm12272_01h_rep1	12272	01h	2	1	1
dm12272_01h_rep2	12272	01h	2	1	1
dm12272_01h_rep3	12272	01h	2	1	1
dm12279_01h_rep1	12279	01h	2	1	1
dm12279_01h_rep2	12279	01h	3	2	1
dm12279_01h_rep3	12279	01h	3	2	1
dm11037_38d_rep1	11037	38d	3	1	2
dm11037_38d_rep2	11037	38d	3	1	2
dm11037_38d_rep3	11037	38d	3	1	2
dm11255_38d_rep1	11255	38d	3	1	2
dm11255_38d_rep2	11255	38d	3	1	2
dm11255_38d_rep3	11255	38d	3	1	2
dm12272_38d_rep1	12272	38d	3	1	2
dm12272_38d_rep2	12272	38d	3	1	2
dm12272_38d_rep3	12272	38d	3	1	2
dm12279_38d_rep1	12279	38d	3	1	2
dm12279_38d_rep2	12279	38d	3	1	2
dm12279_38d_rep3	12279	38d	3	1	2

Supplementary Table 2: Metadata for WTC11 experiment

Sample	Library Prep	Platform	Run Accession	Rep	Biosample	File Accession
WTC11	dRNA	ONT	ENCSR392BGY	1	ENCBS944CBA	ENCFF155CFF
WTC11	dRNA	ONT	ENCSR392BGY	2	ENCBS593PKA	ENCFF771DIX
WTC11	dRNA	ONT	ENCSR392BGY	3	ENCBS474NOC	ENCFF600LIU
WTC11	cDNA	PacBio	ENCSR507JOF	1	ENCBS944CBA	ENCFF563QZR
WTC11	cDNA	PacBio	ENCSR507JOF	2	ENCBS593PKA	ENCFF370NFS
WTC11	cDNA	PacBio	ENCSR507JOF	3	ENCBS474NOC	ENCFF245IPA
WTC11	cDNA	ONT	ENCSR539ZXJ	1	ENCBS944CBA	ENCFF263YFG
WTC11	cDNA	ONT	ENCSR539ZXJ	2	ENCBS593PKA	ENCFF023EXJ
WTC11	cDNA	ONT	ENCSR539ZXJ	3	ENCBS474NOC	ENCFF961HLO